

# Pangaean climate during the Early Jurassic: GCM simulations and the sedimentary record of paleoclimate

MARK A. CHANDLER\* *Lamont-Doherty Geological Observatory, Department of Geological Sciences, Columbia University, Palisades, New York 10964*

DAVID RIND }  
RETO RUEDY } *Goddard Institute for Space Studies, 2880 Broadway, New York, New York 10025*

## ABSTRACT

Results from new simulations of the Early Jurassic climate show that increased ocean heat transport may have been the primary force generating warmer climates during the past 180 m.y. The simulations, conducted using the general circulation model (GCM) at the Goddard Institute for Space Studies, include realistic representations of paleocontinental distribution, topography, epeiric seas, and vegetation, in order to facilitate comparisons between model results and paleoclimate data. Three major features of the simulated Early Jurassic climate include the following. (1) A global warming, compared to the present, of 5 °C to 10 °C, with temperature increases at high latitudes five times this global average. Average summer temperatures exceed 35 °C in low-latitude regions of western Pangaea where eolian sandstones testify to the presence of vast deserts. (2) Simulated precipitation and evaporation patterns agree closely with the moisture distribution interpreted from evaporites, and coal deposits. High rainfall rates are associated primarily with monsoons that originate over the warm Tethys Ocean. Unlike the "megamonsoons" proposed in previous studies, these systems are found to be associated with localized pressure cells whose positions are controlled by topography and coastal geography. (3) Decreases in planetary albedo, occurring because of reductions in sea ice, snow cover, and low clouds, and increases in atmospheric water vapor are the positive climate feedbacks that amplify the global warming.

Similar to other Mesozoic climate simulations, our model finds that large seasonal temperature fluctuations occurred over mid-

and high-latitude continental interiors, refuting paleoclimate evidence that suggests more equable conditions. Sensitivity experiments suggest that some combination of ocean heat transport increase, high levels of CO<sub>2</sub>, and improved modeling of ground hydrological schemes may lead to a better match with the geologic record. We speculate, also, that the record itself is biased toward "equable" climatic conditions, a suggestion that may be tested by comparing GCM results with more detailed phytogeographic analyses.

## INTRODUCTION

Paleoclimate simulations using three-dimensional general circulation models (GCMs) have, generally, been concentrated on two geologic intervals: the Pleistocene Epoch (COHMAP Members, 1988; Kutzbach and Guetter, 1986; Kutzbach and Street-Perrott, 1985; Manabe and Broccoli, 1985; Manabe and Bryan, 1985; Rind, 1987a) and the Cretaceous Period (Barron, 1980; 1985; Barron and others, 1981; Barron and Washington, 1982a, 1982b, 1984; Fleming, 1983; Oglesby and Park, 1989; Rind, 1986). At the most basic level, these two periods represent end-member climates with respect to surface air temperature. Thus, not incidentally, they are scenarios which provide useful information to climate modelers interested in the phenomenon of global warming. Numerous other factors, however, contribute to the prominence of these time periods in simulation studies.

The Pleistocene geologic record is abundant with available paleoclimate data, including continuous sediment and isotopic records from ocean cores, large numbers of geochemical, sedimentary, and vegetational records, and even samples of ancient air from ice cores (see review by Bradley, 1985). Such detailed data are important aids in accurately constructing model boundary conditions and in validating model re-

sults. Pleistocene model-data comparisons are also made easier by the fact that the geographic positions of the continents have changed little over the past 2 m.y., thus making direct comparisons with the current climate much simpler. In addition, the Pleistocene is clearly of great interest because of the extreme climatic changes associated with ice-age fluctuations, including changes in ice-sheet and sea-ice extent, variations in the Indian and African monsoons, shifts in low-latitude desert regions, and large-scale ecosystem migrations.

Cretaceous paleoclimate data, although not nearly as plentiful as that from the Pleistocene, exist in large amounts compared to other Mesozoic periods (see review by Crowley, 1983). This results partially because, during this time of relatively high sea level, abundant shallow-marine and associated nearshore deposits were formed on or near the continents. Cretaceous deposits, furthermore, contain an abundance of economically important hydrocarbon resources, as well as evidence of important geologic events such as the rise to prominence of the angiosperms, the culmination of the age of the dinosaurs, and evidence for an asteroid impact that may have led to the mass extinction of fauna at the end of the period. In addition, the contrasts that exist between the Cretaceous and our Pleistocene world make it a target of scientific curiosity: the paleogeography was different from the present (Smith and Briden, 1977; Ziegler and others, 1983); the paleobiology was unique (Doyle, 1987; Hallam, 1975, 1985; Wolfe and Upchurch, 1987; Ziegler and others, 1987); solar luminosity was probably reduced (Newman and Rood, 1977); and, by most analyses, no permanent land ice existed (Barron and others, 1981; Barron and Washington, 1982b; Frakes, 1979; Hallam, 1985; see Frakes and Francis, 1988, for an opposing view). In addition, the evidence for a warmer climate has led to hypotheses about increased atmospheric trace

\*Present address: NASA/GISS, 2880 Broadway, New York, New York 10025.

gases (Arthur and others, 1985; Barron, 1985; Berner and Landis, 1987; Schneider and others, 1985) and changes in ocean heat transport (Rind and Chandler, 1991).

Recently, research has been directed toward two additional pre-Pleistocene paleoclimate scenarios, including (1) the Eocene (Barron, 1987; Rind and Chandler, 1991; Sloan and Barron, 1990), with climate problems similar to those of the Cretaceous, with the added curiosity that low-latitude cooling may have occurred concurrently with the high- and mid-latitude warming (Shackleton and Boersma, 1981); and (2) the supercontinent scenario (Crowley and others, 1987, 1989; Kutzbach and Gallimore, 1989), in which all (Pangaea) or many (Gondwana and Laurasia) of the continents formed a contiguous landmass. The reasons for interest in Early Jurassic supercontinent climates are also similar to those for the Cretaceous climate. Paleogeography and vegetation were very different from the present, whereas sea surface temperatures (SSTs), atmospheric composition, and solar insolation were probably altered as well. Like the Eocene, the Early Jurassic, Pangaeon climate exhibits complex changes that have very different consequences at low and high latitudes. Diverse floral assemblages at high latitudes and the lack of glacial evidence indicate that the polar regions were warmer and wetter than they are today, a ubiquitous signal in the Mesozoic and early Cenozoic record (see review by Hallam, 1985). Vast expanses of evaporites and eolian dune deposits at low latitudes, however, indicate the presence of tropical warmth and aridity during the Jurassic in excess of any other Phanerozoic time period (Gordon, 1975). Expanded interest in Jurassic climates has also appeared in the climate-modeling community since the prediction was made that low- to mid-latitude aridity will occur in the next century concurrent with global warming. Finally, interest in supercontinental processes has culminated in an international research initiative dealing with Pangaea which is organized by the Global Sedimentary Geology Program (GSPG), and which will include studies of Pangaeon climate.

This paper presents the results of a Pangaeon climate simulation conducted using one version of the Goddard Institute for Space Studies' general circulation model (GISS GCM). The simulation is designed to approximate the climate of the Early Jurassic (Pliensbachian) Epoch. We have used boundary and initial conditions that are based on the best available estimates from the geologic record, and we have strived to include all conditions which are significant on the spatial scale used by the GCM. The

conditions are represented in far greater detail than in previous experiments and include continental reconstructions, topography, epeiric sea extent, vegetation distributions, and sea surface temperatures. These improved representations of surface conditions in the GCM are intended to provide simulated climate results that can be more critically compared to paleoclimate data from the geologic record.

### THE GISS GENERAL CIRCULATION MODEL

The GISS GCM is a three-dimensional global climate model that can be run using a variety of grid resolutions, ocean models, ground hydrology schemes, and cloud parameterizations. A complete description of the GISS GCM and the results of a current climate simulation (referred to in the climate literature as a "control run") may be found in Hansen and others (1983, model II). The version we use for the Early Jurassic simulation operates with a  $7.83^\circ \times 10^\circ$  (latitude  $\times$  longitude) horizontal resolution with nine vertical atmosphere layers plus two ground hydrology layers. It solves the fundamental physical equations for the conservation of mass, energy, momentum, and moisture, as well as the equation of state which relates the atmospheric pressure, density, and temperature. The GISS GCM includes both seasonal and diurnal cycles in its temperature calculations and its radiation computations take into account aerosols, cloud particles, and all significant atmospheric gases, including trace gases (carbon dioxide, methane, etc.). The cloud parameterization predicts both large-scale and convective cloud cover, and precipitation may occur from either cloud type when supersaturated conditions exist. In a typical simulation, using specified sea surface temperatures, the GCM is "spun-up" through one annual cycle, after which the principle components of the model are in equilibrium. The results presented here are averages over the final five years of a six-year simulation. Sensitivity experiments that are described in this paper were generally run for between two and five years and used our primary Early Jurassic simulation for their initial state.

### BOUNDARY CONDITIONS FOR THE GISS GCM

The Early Jurassic lasted for  $\sim 20$  m.y., from 208 Ma to 178 Ma (Harland and others, 1990). The continental distribution we use is based on a Pliensbachian reconstruction by Ziegler and others (1983; see their fig. 2), which includes

estimates of paleotopography and the extent of epeiric seas. Like the Cretaceous (and other periods of the Mesozoic and early Cenozoic) a great deal of the paleoclimate data from the Jurassic indicate that the climate at that time was warmer than it is at the present. High latitudes in particular are conspicuous because they lack glacial deposits and yield evidence of diverse fossil flora (Hughes, 1973), which suggest that temperatures near the poles were probably amplified more than at lower latitudes. Even though the Cretaceous is generally characterized as more humid than the present, extensive evaporites and eolian sandstones suggest that the Jurassic Period was considerably more arid than the present climate (Arkell, 1956; Frakes, 1979; Gordon, 1975; Hallam, 1985; Hubert and Mertz, 1984; Kocurek and Dott, 1983). Based on the latitudinal extent of evaporite deposits, the Early Jurassic was probably not as dry as the Middle and Late Jurassic Epochs; however, it was selected for this experiment on the basis of several additional advantages which are discussed below.

Table 1 lists the boundary and initial conditions that must be assigned in order to initiate the GISS GCM. Figure 1 shows the primary boundary conditions that were changed in order to simulate the Early Jurassic. The results of the simulation depend not only on the ability of the GCM to model physical climate processes, but also on our ability to provide accurate boundary conditions for the simulation. Assigning boundary conditions is perhaps the most difficult task for paleoclimate simulations, and many limitations of GCM paleoclimate runs are related to our lack of knowledge about past conditions. As the GCMs become more sophisticated, and we begin to investigate paleoclimate patterns on the regional scale, it becomes necessary to provide realistic boundary conditions in order to compare simulation results to the geologic record.

### Paleocontinental Distribution

Figure 1a is a paleocontinental reconstruction for the Pliensbachian Epoch of the Jurassic Period, and Figure 1b shows the Pangaeon land distribution and topography used in our simulation. During the Pliensbachian, southern China collided with Laurasia, and the supercontinent of Pangaea attained its most complete configuration. Pangaea had drifted northward to a position that left the south pole in open waters for the first time since the mid-Ordovician (460 Ma). At this time, Pangaea was arranged nearly symmetrically about the equator with 51.5% of the land area located in the northern hemisphere

TABLE 1. BOUNDARY CONDITIONS REQUIRED BY GISS GCM

1. Continental distribution and topography
2. Terrestrial vegetation type and distribution
3. Extent of inland lakes and epeiric seas
4. Land and sea ice coverage
5. Sea surface temperature distribution
6. Atmospheric trace gas content
7. Orbital parameters
8. Solar radiation incident at top of atmosphere

as compared with 63% today (Parrish, 1985). Overall, the supercontinental landmass extended from 85°N to 80°S and spanned 180° of longitude. The elevations given by Ziegler and others (1983) for this time period were only qualitative, and so we quantified them by assuming that Pangaeian and present-day regions with similar tectonic settings would have similar elevations. The result is that the landmass in our Early Jurassic reconstruction covers 28.7% of the Earth's surface and has an average elevation of 135 m. This can be compared to the continental values used in GISS's current climate simulation, which has 29.1% land coverage with a 233-m average elevation.

The extensive, continuous, and symmetrical land coverage during Early Jurassic time reduces the complexity of simulating and interpreting the modeled paleoclimate. For climate analysis, the one-continent configuration is the most simplistic end member of continental organization. It presents an interesting yet realistic paleogeographic scenario for climate study. In addition, the broad latitudinal extent of the Pangaeian continent yields geologic data that cover a continuous range of latitudes in both hemispheres, providing critical information about equator to pole climate gradients.

#### Ocean Basins and Sea-Surface Temperatures

A corollary to the simplified paleocontinental distribution is the uncomplicated shape of the ocean basin. One large ocean, Panthalassa, covered the globe from pole to pole across a longitudinal extent of 180°. The Tethys Ocean separated northern and southern Pangaea in the east and was an equatorial embayment of the western Panthalassic Ocean (see Fig. 1).

The major effect that oceans have on climate in the GCM arises from their ability to transport heat and to act as a source and sink for H<sub>2</sub>O. The GISS GCM parameterizes moisture and heat transfer from the ocean to the atmosphere based on the SST distribution. The importance of the SST distribution should not be underestimated, because previous paleoclimate modeling studies (Barron, 1987; Rind and Peteet, 1985; Rind and others, 1986; Sloan and Barron, 1990) have indicated that the Earth's climate, especially at tropical latitudes, may be very sensitive to this factor. The errors inherent in supplying the SST field represent a serious limitation to paleoclimate modeling of pre-Pleistocene periods; however, effective full-ocean models are not yet available, and the static mixed-layer oceans used in some GCM experiments generate high-latitude SSTs that are inconsistent with temperature estimates made using the geologic record (Barron and Washington, 1982a). For this reason, simulations that use mixed-layer oceans commonly assign a minimum allowable SST in order to maintain warm polar region tempera-

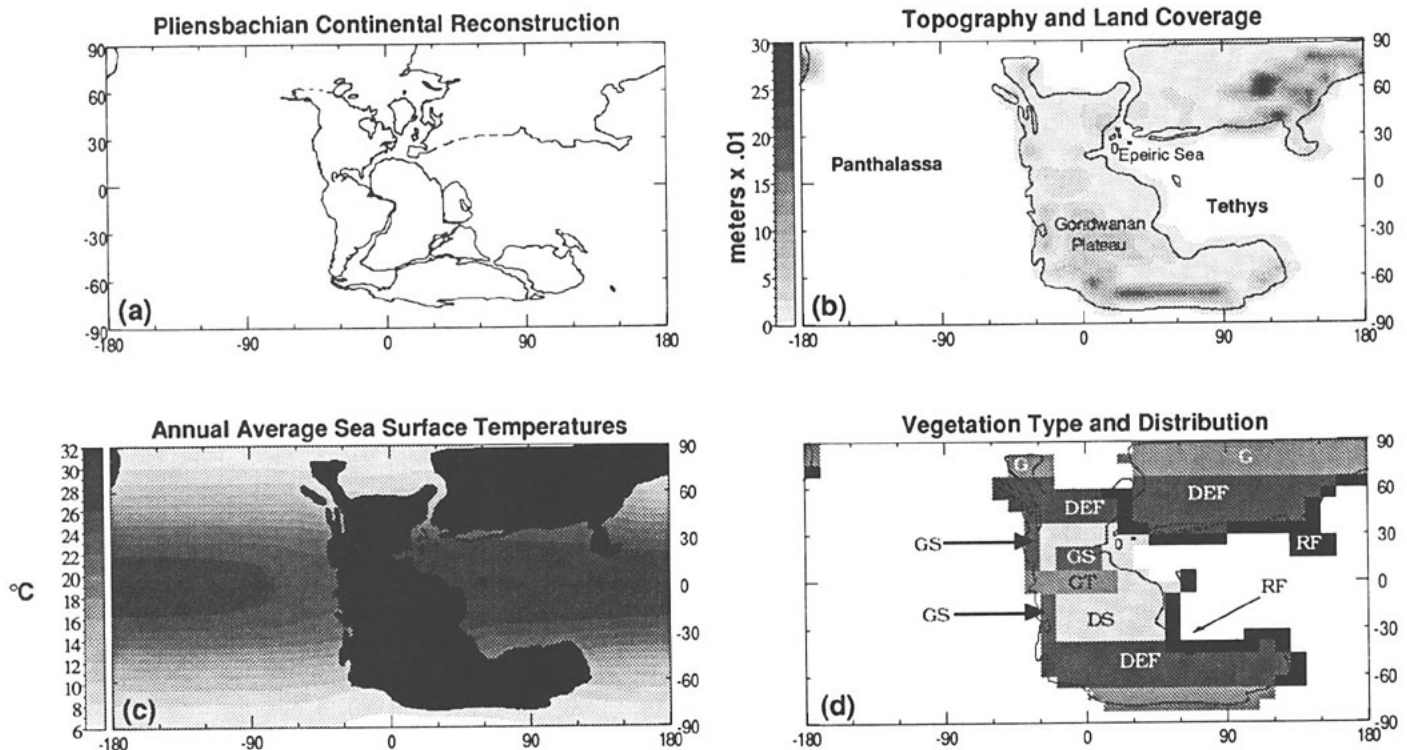


**Figure 1.** Early Jurassic boundary conditions used in GISS GCM. (a) Paleogeographic reconstruction of the Pliensbachian Epoch. The reconstruction is the most recent version produced by the Paleogeographic Atlas Project (D. Rowley and others, unpub. data). (b) Land coverage and topography. (c) Sea-surface temperatures (SSTs). (d) Terrestrial vegetation. The vegetation categories include desert (DS), savannah-type vegetation (G), savannah with scattered shrubs (GS), savannah with scattered trees (GT), mixed deciduous-evergreen forest (DEF), and rainforest (RF).

tures. In our simulation, we use a specified SST distribution which adjusts daily, thus accounting for seasonal temperature fluctuations. As Barron and Washington (1982b) pointed out, this method of simulating past polar warmth implies that increased ocean heat transports were a significant component of the climate system, an important point which we discuss below.

The Early Jurassic SST distribution, shown in Figure 1b, is an estimate based on data from numerous sources. These include the resources of the Paleogeographic Atlas Project (A. M. Ziegler, 1991, personal commun.) and the compilations of Arkell (1956), Brenchley (1984), Frakes (1979), and Hallam (1975). The constraints on our SST estimates are (1) no high-latitude ice sheets, (2) broad latitudinal extent of warmer climate vegetation types and high-diversity floral assemblages located at high-latitude coastal positions, (3) greater latitudinal extent of hermatypic corals and greater diversity of other marine invertebrates in the Tethys region, (4) regionally extensive evaporite and carbonate deposits, and (5) estimates of paleocurrents, taking into account the Coriolis force and continental barriers. The reliability of the available oxygen-isotope measurements is questionable (see Hallam, 1975, for a review) and such quantitative data are too few and too variable to be seriously useful for determining the SST distribution for the Early Jurassic; however, we point out that the SST distribution we use is generally consistent with the minimum SST estimates (most positive  $\delta^{18}\text{O}$  values) that were made by Stevens and Clayton (1971) using isotopes.

As the single-basin ocean configuration decreases the complexity of the wind-driven ocean circulation, this may reduce the error in the estimates of SST distribution. Yet, thermohaline circulation changes, potentially of equal or greater importance, are not explicitly considered in this study. Major features of our specified SST field include warm polar waters (seasonal range = 3.5 °C to 9.5 °C), a low equator-to-pole temperature gradient (22.2 °C), and an east-west equatorial temperature gradient (from 25 °C in the east Panthalassic to 32 °C in the west Tethys). Globally averaged, our specified Jurassic ocean is 3.0 °C warmer than the SSTs used in the current climate GISS GCM experiments, which are taken from observed climatology.

### Vegetation

Several studies have shown the importance of including more realistic representations of vegetation in GCMs (Emmanuel and others, 1985;

Hansen and others, 1983, 1984; Rind, 1984; Rind and others, 1990), and numerous vegetation schemes, of varying complexity, have been applied to the problem (Abramopoulos and others, 1988; Dickinson, 1984). The simplest schemes account only for vegetation's effect on surface albedo; however, other properties of plants, such as their influence on soil moisture, surface runoff, and evapotranspiration (the transport of water from the soil to the atmosphere), play important roles in regulating continental climates (Rind, 1982, 1984; Rind and others, 1990; Sud and Smith, 1985; Thornthwaite, 1948). These additional properties are included in the GISS GCM's ground hydrological scheme and are dependent upon specified vegetation types. The GISS GCM includes eight categories of vegetation which were condensed from a larger global data base (Matthews, 1984, 1985). Each vegetation category is used to define (1) surface albedo (adjusted seasonally), (2) the water-holding capacity of the ground layers (soil moisture), and (3) the degree to which snow reflectivity is masked (Hansen and others, 1983).

The vegetation distribution used in the Early Jurassic simulation is shown in Figure 1c. Paleofloral distributions were constructed using data from several sources (Filatoff, 1975; Hallam, 1975, 1985; Hughes, 1973; Termier and Termier, 1960; Vakhrameev, 1965, 1970; Wesley, 1973). The Jurassic floras were assigned to the GCM's vegetation categories based upon fossil plant morphologies and inferences about their functional properties as compared with modern flora (B. Cornet, 1989, personal commun.; E. Matthews, 1989, personal commun.; A. M. Ziegler, 1989, personal commun.). In addition to our original Jurassic experiment, we ran two other simulations in which we modified the vegetation distributions in order to test the climatic sensitivity to such changes. The first of these simulations applied a uniform vegetation over all continental regions, whereas the second tested the sensitivity of a low-latitude coastal climate to vegetation change.

### Land and Sea Ice

The geologic record contains no definitive tilites or glacial-marine deposits of Early Jurassic age (Hallam, 1985); thus, no conclusive evidence exists for the presence of permanent land or sea ice during this epoch. This evidence does not rule out the possibility of seasonal ice formation, which may account for potentially ice-raftered deposits of Middle Jurassic age in northeastern Siberia (Frakes and Francis, 1988).

Diverse fossil floras, some of which have modern relatives living in regions that rarely experience freezing temperatures, are found in coastal deposits of Greenland and Antarctica at Early Jurassic paleolatitudes above 60° (Barnard, 1973; Frakes, 1979; Hallam, 1985; Wesley, 1973). Ongoing paleofloral research should give us more detailed paleoclimate information from these high-latitude sites (for example, R. Spicer and J. Parrish, 1990, personal commun.) and improve our understanding of the polar seasonal temperature variations that existed during the Mesozoic. Although we do not begin our simulation with snow cover, snow is formed by the GCM, and it does accumulate over portions of Pangaea during the winter months.

### Atmospheric Composition and Solar Radiation

In this simulation, the atmospheric composition and solar radiation are set at present-day values, and current orbital parameters are used to calculate the seasonal and latitudinal radiation distribution. The forcing for climate change originates, primarily, from the specified SSTs, land distribution changes, and ice-sheet changes.

Although geologic evidence suggests that Milankovitch-type variations did occur during the Early Jurassic (Olsen, 1986), our choice of modern orbital parameters is arbitrary because the results are compared with paleorecords that span 20 m.y., accumulating under multiple Earth-Sun arrangements. Solar-evolution theory suggests that solar luminosity has increased through time (Newman and Rood, 1977), and many speculations have been raised regarding increased CO<sub>2</sub> as a forcing mechanism for Mesozoic warming. Unfortunately, there is no method to measure trace gases or solar radiation from the Jurassic record, and as a result, sensitivity experiments are commonly used to investigate the climate effects of solar radiation and atmospheric composition changes (for example, Barron and Washington, 1985; Overpeck and others, 1989). Some previous sensitivity experiments have used explicit means of including CO<sub>2</sub> (Barron and Washington, 1985), whereas others employed solar-radiation changes to approximate CO<sub>2</sub> increase (Kutzbach and Gallimore, 1989). We have conducted four Early Jurassic experiments with increased CO<sub>2</sub> levels (2×, 3×, 4×, and 6×), using the explicit method; however, specifying SSTs minimizes the climate effects by previously accounting for many of the CO<sub>2</sub>-induced feedbacks (sea-ice decrease, water-vapor increase), thus limiting the CO<sub>2</sub> ef-

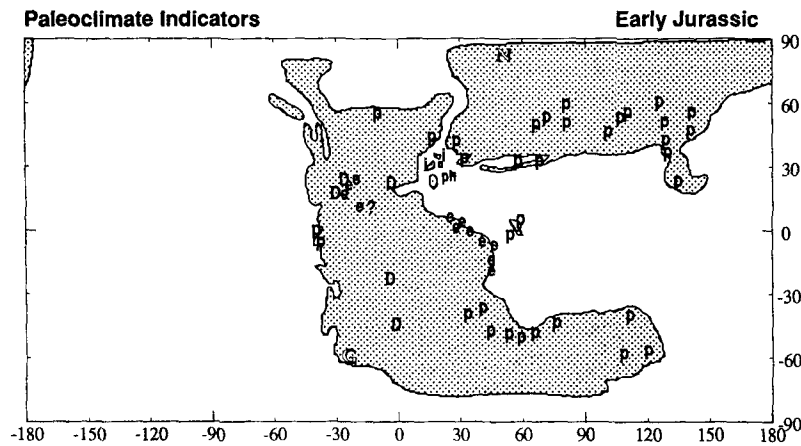


Figure 2. Global distribution of Early Jurassic paleoclimate indicators. Evaporite (e); eolian "dune" sandstone (D); peat or coal (p); ironstone (i); phosphate (Ph); Novosibirskiy paleoflora (N); Graham Land paleoflora (G); Novosibirskiy and Graham Land are the highest known latitudinal positions of Early Jurassic paleofloras.

fect to direct radiative heating (Sloan and Barron, 1990). It was initially our intention to use the radiation imbalance of the model, generated by including artificially warm SSTs (see below), to estimate past amounts of  $\text{CO}_2$ ; however, for reasons discussed in this paper, such experiments were not warranted.

#### Paleoclimate Data

Figure 2 shows a map of climatically indicative sedimentary deposits from the Early Jurassic Epoch which are used to test model results. The data were summarized from the paleoclimate dataset compiled by the Paleogeographic Atlas Project at the University of Chicago. Interpretations of paleo-temperatures are generally made from paleofloral, paleofaunal, and glacial deposits (or the lack thereof); peat and coal deposits, evaporites, and eolian deposits provide most of the information about atmospheric moisture. Data such as these are the only true means for testing GCM paleoclimate simulations; however, the information they provide is semiquantitative at best, limiting our ability to test the model's quantitative accuracy (Rind, 1990). Assigning boundary conditions and testing model results are also limited by the lack of geologic data over large regions of Pangaea. Ultimately, the goal of paleoclimate modeling is to help to fill these gaps and to quantify the paleorecord, a formidable task considering the sparsity of the geologic record and the complexities involved in quantifying paleoclimate data.

### THE EARLY JURASSIC SIMULATION: GLOBAL RESULTS

#### Early Jurassic Warmth: A Self-Sustaining System?

The warm climate of the Early Jurassic, as simulated in this experiment, turns out to be self-sustaining. The global, annually averaged surface-air temperature in the Early Jurassic is  $5.2^\circ\text{C}$  greater than that of the control experiment, although the vertically integrated air temperature increases by only  $3.4^\circ\text{C}$  (Table 2). These figures are approximately equivalent to the warming generated by a doubling of  $\text{CO}_2$  in the GISS GCM (Hansen and others, 1984), the major difference being that the vertically integrated temperature increase in the Early Jurassic is not as great in proportion to the surface-temperature increase. The greater surface warming is a consequence of using a surface forcing mechanism, namely warmer SSTs, to warm the atmosphere. Specifying warmer high-latitude SSTs also implies that the oceans were transporting greater amounts of heat poleward in the Jurassic than they do today.

Another consequence of specifying warmer SSTs is that the amount of thermal radiation generated by the Earth increases, leading to an imbalance in the net radiation (NR) of the planet, as measured at the top of the atmosphere. The net radiation is given by the simple equation

$$\text{NR} = (\text{ISR}) - (\text{ETR}) + (\text{CO}_2\text{TR})$$

TABLE 2. SELECTED CLIMATE VARIABLES SIMULATED BY THE GISS GCM FOR EARLY JURASSIC AND CURRENT CLIMATES

Climate variable	Simulation values	
	Early Jurassic	Current
<i>Temperature</i>		
Surface air temperature ( $^\circ\text{C}$ )	18.7	13.5
Vertically integrated air temperature ( $^\circ\text{C}$ )	18.5	-21.9
Sea surface temperature ( $^\circ\text{C}$ )	22.4	19.4
<i>Radiation</i>		
Net radiation ( $\text{W}\cdot\text{m}^{-2}$ )	11.9	7.9
Incident solar radiation ( $\text{W}\cdot\text{m}^{-2}$ )	341.9	342.3
Exiting thermal radiation ( $\text{W}\cdot\text{m}^{-2}$ )	240.9	231.5
Total solar radiation absorbed ( $\text{W}\cdot\text{m}^{-2}$ )	252.8	239.4
Solar radiation absorbed at surface ( $\text{W}\cdot\text{m}^{-2}$ )	185.2	172.9
Planetary albedo (%)	26.1	30.5
Surface albedo (%)	9.3	12.1
Atmospheric albedo (%)	21.2	25.1
<i>Global cloud cover</i>		
Total cloud cover (%)	46.2	51.6
Low-level clouds (%)	29.1	36.4
Mid-level clouds (%)	16.9	19.7
High-level clouds (%)	28.6	28.8
Supersaturated clouds (%)	39.1	44.3
Moist convective clouds (%)	12.2	13.7
Moist convective cloud depth (mb)	439.7	391.4
<i>Hydrological cycle variables</i>		
<i>Global values</i>		
Snow cover (%)	4.80	10.40
Precipitation ( $\text{mm}\cdot\text{day}^{-1}$ )	3.25	3.10
Evaporation ( $\text{mm}\cdot\text{day}^{-1}$ )	3.24	3.09
Potential evaporation* ( $\text{mm}\cdot\text{day}^{-1}$ )	15.60	12.20
Moist convective precip. ( $\text{mm}\cdot\text{day}^{-1}$ )	3.10	2.85
Large-scale cloud precipitation ( $\text{mm}\cdot\text{day}^{-1}$ )	0.15	0.26
Relative humidity (%)	46.00	45.00
Absolute humidity ( $10^{-5}\text{kg H}_2\text{O} / \text{kg air}$ )	286.20	239.60
<i>Values over land only</i>		
Large-scale clouds (%)	39.70	43.80
Moist convective clouds over land (%)	8.40	10.40
Moist convective cloud depth (mb)	421.30	409.90
Moist convective precipitation ( $\text{mm}\cdot\text{day}^{-1}$ )	1.95	2.33
Large-scale cloud precipitation ( $\text{mm}\cdot\text{day}^{-1}$ )	0.27	0.26
Precipitation ( $\text{mm}\cdot\text{day}^{-1}$ )	2.23	2.60
Evaporation ( $\text{mm}\cdot\text{day}^{-1}$ )	1.59	1.90
<i>Values over ocean only</i>		
Precipitation over ocean ( $\text{mm}\cdot\text{day}^{-1}$ )	3.67	3.45
Evaporation over ocean ( $\text{mm}\cdot\text{day}^{-1}$ )	3.91	3.82

\*Model generated values of potential evaporation are not calculated in a manner similar to the empirical formulas used in common bioclimatic schemes. Therefore, this variable is meaningful only for comparison with other model-generated potential evaporation values.

where ISR is the incoming solar radiation, ETR is the exiting thermal radiation, and  $\text{CO}_2\text{TR}$  is the additional radiation trapped when  $\text{CO}_2$  levels are increased. Prior to running the simulation, we expected that the NR would be negative because we artificially increased the thermal radiation exiting the planet, but we did not increase the incoming solar radiation or the amount of atmospheric  $\text{CO}_2$ . Our intention was to compensate for that negative imbalance by increasing atmospheric  $\text{CO}_2$  in subsequent simulations until  $\text{CO}_2\text{TR}$  increased to the point where the model was equilibrated again. Balanc-

ing the warm SSTs using this method, we thought, would produce an Early Jurassic simulation which did not need artificially maintained SSTs and would yield a quantitative estimate of Mesozoic CO<sub>2</sub> levels.

Significantly, and somewhat surprisingly, the natural climate feedbacks in the system (discussed below) balanced the negative net radiation caused by the warm SSTs. This implies that *no additional CO<sub>2</sub> was needed to maintain the Early Jurassic global warmth*. In fact, the net radiation was positive by 4.0 Wm<sup>-2</sup>. This implies that, had we allowed the SSTs to adjust, not only would they maintain their specified temperatures, but they would actually continue to warm until the ocean surface emitted a level of thermal radiation that balanced the positive radiation effect of the feedbacks. As the sensitivity of the GISS GCM yields a 1 °C atmospheric warming for every +1 Wm<sup>-2</sup>, the ultimate warming in the simulation could have been as much as 9.2 °C (5.2 °C plus 4 °C associated with the radiation imbalance).

We defer most of the discussion of these results to Rind and Chandler (1991) and Covey (1991); however, we point out that if these results are valid the Early Jurassic warming can be sustained purely by increasing ocean heat transports, and then many of the warm climates of the past might be explained solely by changes in ocean circulation.

#### Climate Feedbacks Related To Early Jurassic Warming

Two feedbacks are primarily responsible for the above result. First, the elimination of sea and land ice, a result of the warm polar SSTs and the equatorward shift of Antarctica, decreases the surface albedo, allowing more of the Sun's energy to be absorbed by the planet. This increases temperatures at high latitudes and leads to a decrease in the amount of snow accumulation during winter, further reducing surface albedo. Ultimately, global surface albedo was decreased by 2.8% (Table 2) in the Early Jurassic simulation, despite an albedo increase at low latitudes caused by the large, highly reflective desert regions. The second, primary climate feedback involves atmospheric moisture. In the Early Jurassic simulation, absolute humidity (a measure of total atmospheric water content) rose by 19% (Table 2). As atmospheric temperatures increase, the water holding capacity of the atmosphere also increases (see "Clausius-Clapeyron equation," Wallace and Hobbs, 1977). Water vapor is a strong greenhouse gas which resides predominantly at low levels in the atmosphere, trapping heat and raising temperatures near the surface. Previous modeling studies have found that increased water vapor may,

eventually, be the most important cause of future global warming (Hansen and others, 1984), a hypothesis that is supported by findings from the Earth Radiation Budget Experiment (ERBE) (Raval and Ramanathan, 1989). In light of these findings, it is not surprising that the water-vapor feedback seems to have been an important factor in the warm climate of the Early Jurassic.

Secondary effects also play a role in global warming. In the high latitudes, surface temperatures and atmospheric moisture levels rise due to the increase in sensible and latent heat transfer between the open, warm polar waters and the atmosphere. Total cloud cover also decreases significantly (Table 2) due to the increased water-holding capacity of the atmosphere (or perhaps despite it). Simulations of the current climate show that clouds, overall, cool the atmosphere because the reflective properties of low-level clouds outweigh the heat-trapping ability of high-level clouds (Ramanathan and others, 1989a, 1989b). In many warmer climate simulations (that is, Cretaceous, doubled CO<sub>2</sub>), however, low-level clouds tend to decrease more than high clouds, providing a positive feedback that enhances global warming (Barron, 1980; Hansen and others, 1981, 1984; Rind, 1986; Rind and Chandler, 1991). Similarly, in the Early Jurassic simulation, cloud amounts over both land and ocean are reduced at low and middle levels in the atmosphere. Consequently, planetary albedo decreases by nearly 4% (Table 2), adding yet another positive feedback to the atmospheric warming trend.

#### Global Hydrological Cycle

Although the Early Jurassic atmosphere has a higher water-vapor content, the increased atmospheric moisture does not necessarily translate efficiently into increased precipitation. The 19% increase in absolute humidity is accompanied by only a 1% increase in relative humidity because the warmer atmosphere is capable of holding more moisture. Thus, the globally averaged precipitation rate increases by only 0.15 mm/day (4.8%) over the control experiment (Table 2). Global precipitation is linked primarily to the amount of evaporation occurring over the oceans, which depends upon wind velocity, the drag coefficient (which increases with increasing wind velocity), and the temperature difference between the sea surface and the surface air. In the Early Jurassic simulation, the difference between the surface-air temperature and sea-surface temperatures increases slightly. The decrease in global wind velocities, and therefore the reduced drag coefficient, however, offset most of the temperature effect in the model. The result is a relatively minor increase in evapora-

tion (2.4%) over the oceans, thus limiting the precipitation increase.

The GISS GCM includes representations of two types of clouds. Large-scale clouds, similar to those produced by mid-latitude cyclones, and convective clouds. The convective clouds are responsible for about 90% of the global precipitation. Globally averaged, both large-scale and convective cloud amounts decrease in the Early Jurassic simulation compared with the control experiment. Global precipitation from large-scale clouds also decreases by about half; however, convective cloud precipitation increases by almost 10%. Notably, this increase in convective precipitation is unevenly distributed, illustrated by a large increase over the ocean and a significant decline over the continent. This indicates that the net transfer of moisture from ocean to land was much less in the Early Jurassic than at present. In part this result can be attributed to the supercontinent configuration, which increases the mean distance between the continental interior and the ocean. It is important to point out, however, that precipitation over the continents in the GCM is sensitive to the types of vegetation specified for the ground hydrology scheme. The significance of assigning accurate vegetation was demonstrated in a sensitivity experiment in which we replaced the Early Jurassic deserts with grassland hydrology characteristics. In that simulation, continental precipitation was reduced only about one-sixth of the amount that it decreased in the original Early Jurassic run.

In addition to the reduced precipitation, the potential rate of evaporation also increases in the warmer climate, a factor that must ultimately be considered if we wish to fully understand the availability of moisture on the continent. Rind and others (1990) have shown previously that a positive correlation exists between increases in global temperature, potential evaporation, and the occurrence of severe drought in a doubled-CO<sub>2</sub>, warm climate. Similarly, for the warmer Early Jurassic climate, increased potential evaporation could have further exacerbated the drying of the continent indicated by the precipitation reduction. Temperature distributions over Pangaea (see discussion below) suggest that the effect is potentially important, particularly in low-latitude regions. Although the potential evaporation values calculated by GCMs cannot be used directly due to various complexities (Rind and others, 1990), potential evaporation can be estimated using empirical bioclimatic formulas, a method we employ in our study.

#### Global Atmospheric Circulation

In Figure 3a, we show the longitudinally averaged mass stream function which is a diagnos-

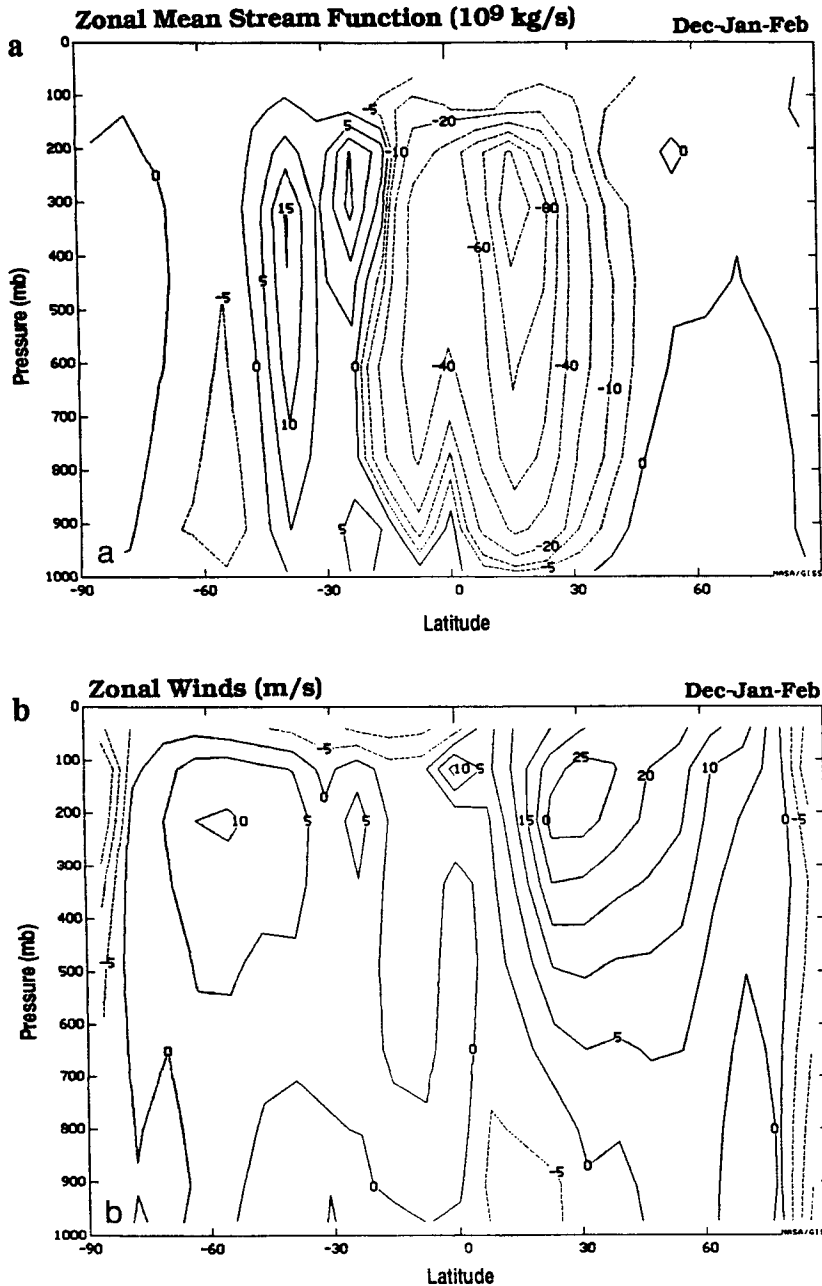


**Figure 3.** Zonally averaged properties of the simulated Early Jurassic general circulation for northern hemisphere winter. The vertical axis is in pressure units (millibars), a common method of representing height above sea level in atmospheric flow diagrams. (a) Zonal mean stream function indicating vertical and north-south air-flow patterns; dashed contours = clockwise flow, solid contours = counter-clockwise flow. (b) Zonal mean winds indicating east-west wind strength; dashed contours = easterly flow, solid contours = westerly flow.

tic used for examining the properties of the general circulation of the atmosphere between the equator and poles. Comparisons with the control experiment (see Rind, 1988) show that the intensity of the low-latitude Hadley cell decreases significantly in the Early Jurassic simulation compared with the present. The decrease in

latent heat flux in the tropics is responsible for most of this reduction. Although the intensity decreases, the Hadley cell in the winter hemisphere expands poleward by a few degrees, and extends farther across the equator into the summer hemisphere. Extension into the summer hemisphere is caused primarily by the deep low-

pressure centers that form over land in summer and which divert the intertropical convergence zone (ITCZ) poleward. The poleward expansion occurs at the expense of the mid-latitude circulation cell (known as the "Ferrel cell"), which is completely absent in the winter hemisphere and is significantly weakened in the summer hemisphere. The Ferrel cell is driven primarily by energy transported in atmospheric eddies (Rind and Rossow, 1984), and the decline in eddy energy suggests a decrease in mid-latitude storms, which are a common example of kinetic energy transported as eddies. Several climate-change simulations have indicated a connection between eddy energy (or storm activity) and the latitudinal temperature gradient (Manabe and Broccoli, 1985; Rind, 1986, 1987a, 1987b). In sensitivity experiments using altered SST gradients with the Early Jurassic boundary conditions, we found further evidence of this correlation. These experiments showed that a 5 °C decrease in SST gradient was accompanied by a 14% drop in eddy energy and a 15 °C gradient reduction dropped eddy energy by an additional 25%.

Prevailing westerly jet streams are the major feature of the Early Jurassic zonal mean wind field (Fig. 3b) and, like today, they are centered at upper levels in the mid-latitudes. The wind intensities are, however, reduced 30% to 50% compared with their present-day counterparts. At subtropical latitudes, the loss of energy in the zonal winds is directly related to the weakening of the Hadley cell, whereas farther poleward, in the upper mid-latitudes, the reduction in eddy-energy convergence (discussed above) is the major cause of zonal wind depletion. The decreased jet intensities in the mid-latitudes are also consistent, through the thermal wind relationship, with the reduction in the vertically averaged latitudinal temperature gradient (see Barron and Washington, 1982a; Holton, 1979). The zonal winds are weakest in the southern hemisphere because the northward displacement of Antarctica, the lack of high-latitude ice, and the warm polar SSTs cause the temperature gradient to be reduced more, compared to the present, in the southern hemisphere. Over the continent, and particularly during winter, the temperature gradient is large, thus strengthening the jet stream (see Fig. 4b).

At high latitudes, the warm polar waters reverse the normal latitudinal temperature gradient, creating polar easterlies at all heights, but over the low-latitude continent, an easterly jet appeared in the Early Jurassic simulation (see Fig. 4b). This jet is the upper branch of a longitudinal circulation cell which is generated by the coupling of intense convection over tropical Pangaea with subsidence over cool waters in the eastern Panthalassic Ocean. On the surface, the

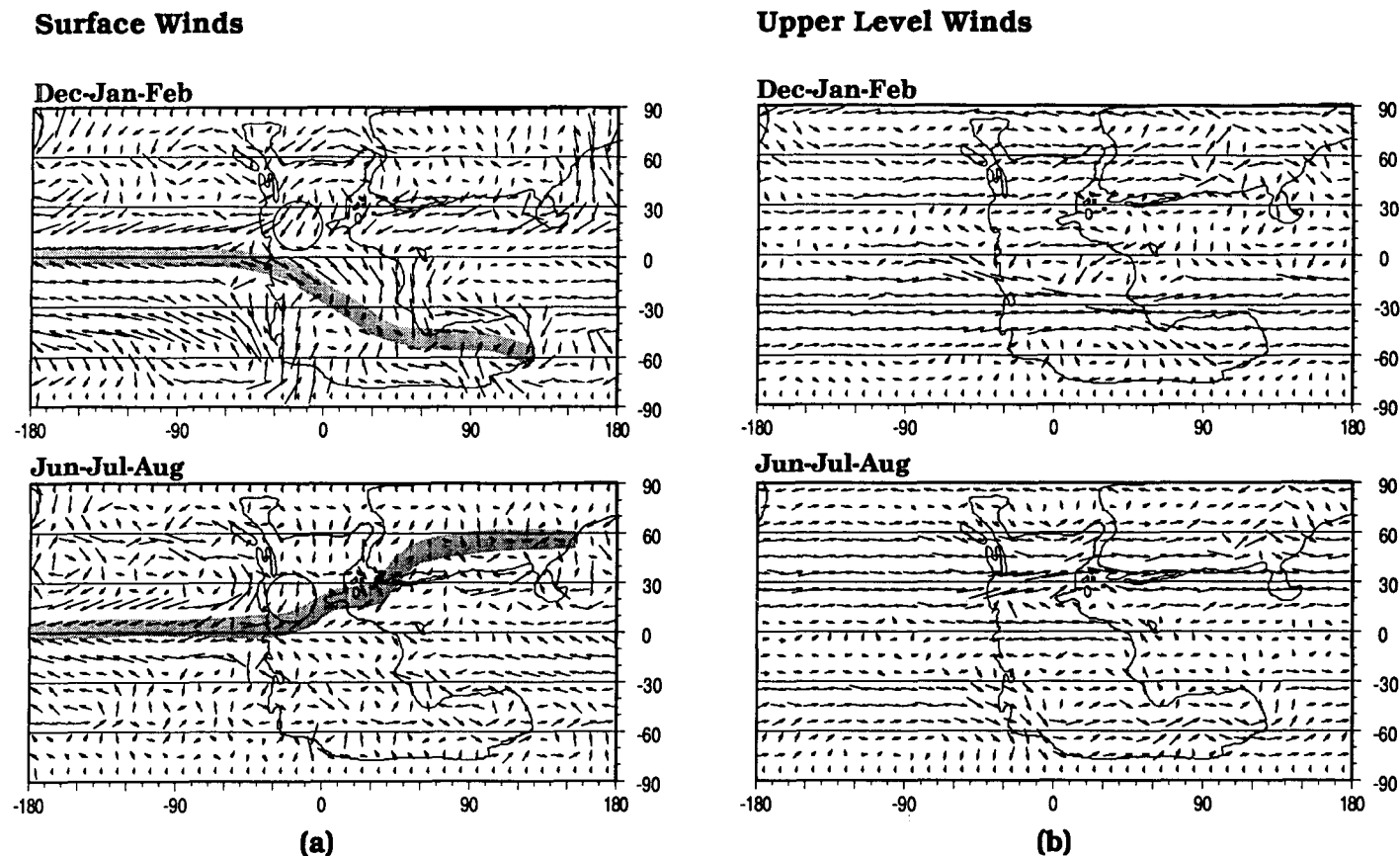


Figure 4. Simulated global distribution of Early Jurassic wind vectors. (a) Surface winds; hatched line indicates approximate position of ITCZ; circled region identifies wind vectors that correspond to region where paleowind estimates are available (see text). (b) Upper-level "jet" winds.

longitudinal circulation cell generates westerly winds across, and just west of, the low-latitude continent. The cyclonic subtropical circulation over southern Pangaea adds to this westerly wind flow, and together the two effects reverse the normal, trade-wind pattern (see Fig. 4a) across the continent. Although winds over the oceans reveal a typical trade-wind pattern, these low-latitude westerlies are strong enough to affect the zonal average.

#### THE EARLY JURASSIC SIMULATION: REGIONAL RESULTS

The regional expression of climate depends upon multiple feedbacks, just as does the globally averaged climate. Regional patterns, however, are controlled to a greater extent by features such as geography and topography, the extent of epeiric seas, sea-surface temperatures, and the vegetation distribution. Glaciation and sea ice are also prominent controls on regional climates, although in the Early Jurassic simulation, they are conspicuous only by their absence.

#### Western Pangaea: The Low-Latitude Continent

Surface-air temperatures are warmest in the low latitudes over the continent with monthly averaged maxima in the subtropical regions (Fig. 5). These maxima are in excess of 35 °C and result from a combination of high solar insolation in the subtropics and the low heat capacity of the continent. Average summer temperatures that exceed 25 °C extend well into the mid-latitudes, 10° to 20° farther poleward than in the present-day climate. The warm surface temperatures create instability in the atmosphere, generating deep low-pressure cells during summer in the subtropics of western Pangaea (Fig. 6). Colder winter temperatures maximize the atmospheric stability, thus the summer low-pressure cells alternate seasonally with winter high-pressure cells. The high-pressure centers are located 15° to 20° poleward of the peak lows in response to the winter cooling at high latitudes.

The pressure cells influence the surface wind

flow (Fig. 6a) over the continent to the extent that trade winds, which are well developed throughout the year over the ocean, are severely modified over the continent (see discussion above). The surface flow is more intense in the southern hemisphere, responding to the enhanced temperature and pressure fields over the elevated Gondwanan Plateau. A similar process occurs over the Tibetan Plateau in the current climate (Druryan, 1982a, 1982b; Ruddiman and Kutzbach, 1989).

One consequence of this surface-flow pattern is that very little moisture is directed toward the interior of the continent in low latitudes. Therefore, despite the presence of low pressure in subtropical regions, the lack of moisture convergence results in a reduction of total cloud cover across western Pangaea (see Table 2). Decreased storm activity, related to the decrease in the vertically averaged equator-to-pole temperature gradient, further reduces mid-latitude cloud cover. The greatest reductions occur in low-level clouds (Fig. 7a), although moist convective cloud amounts decrease throughout the tropics

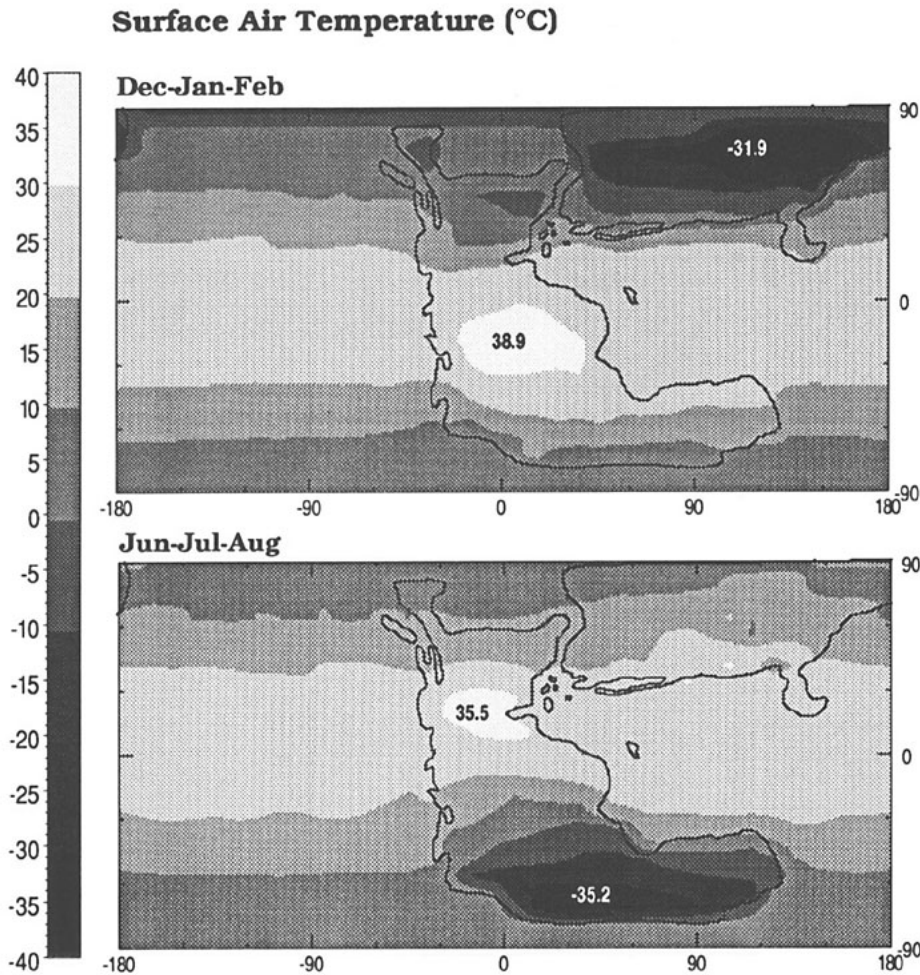


**Figure 5.** The simulated global distribution of Early Jurassic surface-air temperatures. Insolation forcing generates the greatest heating in the subtropical and tropical regions of western Pangaea. Extremely cold winter temperatures over high-latitude, high-elevation regions of the continent result in annual temperature ranges that exceed 45 °C.

as well. High-level clouds (Fig. 7b) are reduced on the western side of the continent but are increasingly present toward the Tethys Ocean and within the tropical zone, where warm SSTs and high evaporation rates provide moisture to the atmosphere, creating the conditions for deep convection, which transports the moisture to high altitudes. The reduction of low clouds reduces the albedo over western Pangaea, which acts as a positive feedback to warming in that region. The lack of clouds also implies a similar lack of rainfall in the region, and the precipitation results shown in Figure 8a are consistent with this suggestion. Vast regions in the western low latitudes of Pangaea receive less than 250 mm of rain annually (0.7 mm/day). Generally, regions receiving so little rain cannot support vegetation, and this limit is commonly used to define arid zones (Bates and Jackson, 1980; Glennie, 1987).

Despite the similarity between the hemispheric patterns, a substantial degree of asymmetry exists, caused by land-sea distribution and topographic differences. The epeiric seaway that extends northwestward from the Tethys Ocean acts to narrow the longitudinal extent of the continent in the northern subtropics (see Fig. 1). This imparts a more maritime climate to that region, resulting in subdued seasonal pressure and temperature variations. South of the equator, the higher elevation of the Gondwanan Plateau enhances the seasonality. The plateau intensifies the cyclonic flow above the subtropical low in summer and pulls large amounts of moisture off the warm low-latitude Tethys Ocean, generating monsoon conditions over coastal regions of the southwest Tethys. Coastal topography and the Hadley circulation reinforce the rising motion caused by heating over the continent in winter, resulting in increased cloud

formation and higher precipitation rates in a 1,500-km-wide zone along the southwestern Tethys coast. On the opposite side of the Gondwanan Plateau, along Pangaea's west coast, a similar surface-flow pattern generates increased precipitation. Maximum precipitation values, however, are lower than on the Tethys coast because cool SSTs in the eastern Panthalassic Ocean reduce evaporation and decrease convection in this region.

#### Northern Pangaea: The Middle and High Latitudes

The climatic patterns over the northern Pangaea are controlled, to a large degree, by the presence of the epeiric seaway and by orography. Sea-level pressure contours (see Fig. 6) parallel the shoreline of the epeiric sea, indicating its role in separating the northern hemisphere pressure centers. This effect is most evident during winter where the warm SSTs inhibit the formation of high pressure over the region surrounding the seaway. In marked contrast, the colder temperatures over the eastern portion of northern Pangaea stabilize the continental air masses, generating high pressures. To the west of the seaway, anticyclonic circulation around a weak high generates northeasterly winds which join the trade-wind circulation in the subtropics. As these winds cross the epeiric sea, they evaporate large quantities of water from the surface (Fig. 8b), which condenses as the flow reaches the coastline and rises over the colder continental air mass. Figure 8a shows the extremely high precipitation rates (up to 8 mm/day) that are generated in this manner on the southwest coast of the epeiric sea. During the summer, high pressure over the polar ocean and low pressure over the western Tethys and low-latitude Pangaea create a north-south pressure gradient which generates southerly surface winds along the axis of the epeiric seaway. Despite the warmer sea-surface temperatures and high evaporation rates, summer precipitation rates are much lower than in winter because of the relative lack of onshore flow.

East of the epeiric sea, the continental climate is controlled primarily by pressure cells that develop over the high topography on the far eastern portion of the peninsula. During winter, the reduced seasonal insolation, the high elevations, and the expansive landmass create extremely cold temperatures north of 45°N (see Fig. 5). Approximately 75% of the northern peninsula is covered by below-freezing temperatures throughout the winter, with the coldest surface temperatures (-30 °C) located over the high-latitude mountains in the northeast. The resulting high pressure and stability of the winter air mass in

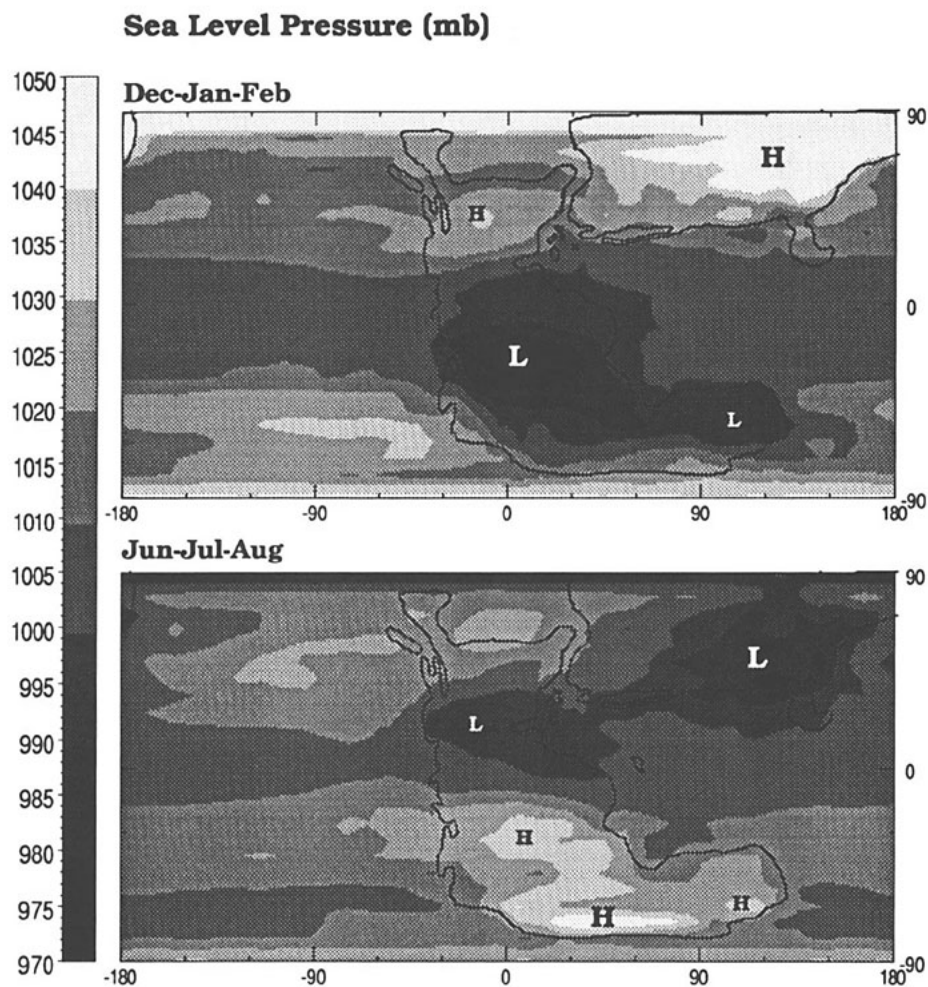


**Figure 6. Simulated global distribution of Early Jurassic sea-level pressure. Winter high-pressure cells alternate with summer low-pressure cells over the continent. The cells are, in general, localized by surface heating, which is affected by latitude, topography, and continentality. Subpolar low-pressure cells develop over the ocean; however, the subtropical high-pressure zone, typically present in the current climate, is absent.**

northern Pangaea, along with the low moisture-holding capacity of the cold air, are responsible for the weak winds and the low rate of winter precipitation across the northern interior.

Increased solar radiation during summer intensifies heating at the surface, and summertime temperatures range from 10 °C near the pole to 30 °C in the south-central portion of the peninsula. The warm temperatures generate a diffuse low-pressure zone over the continent that deepens above the higher elevations in the east. Despite the dominance of one large low-pressure system, the summertime precipitation field over the northern interior is divided into three longitudinal segments. The western segment is delineated by the epeiric sea to the west and the ancient Ural Mountains to the east. In this region, surface and upper-level winds advect moisture from the epeiric sea and Arctic Ocean up to

2,500 km into the peninsula. Eventually, distance from the source and increasing elevation prevent further penetration into the continental interior. East of the Urals, in the central segment of the continent, elevation drops, and the air subsides and warms, suppressing condensation across the south-central lowlands and south-central Tethys coast. In the north-central region, northerly winds, generated by the low pressure farther east, force cooler, more stable air into the central lowlands, enhancing the aridity of the continental interior. Seasonally averaged summer temperatures in the interior reach 30 °C in some grid boxes. These high temperatures result, in part, from high sensible heat fluxes which develop because coastal mountain ranges block moisture from reaching this region, thus decreasing evaporative cooling of the surface. Most of the moisture in the far eastern portion of north-

ern Pangaea is supplied by the advection of moisture from the Panthalassic and Tethys Oceans, whereas local precipitation maxima result as these moisture-laden air masses move up the stoss sides of individual mountain ranges.

Seasonally alternating cyclonic and anticyclonic circulations are established around the eastern pressure centers and have a particularly important effect on the southeast Asian portion of northern Pangaea. That region is geographically situated such that, during winter, anticyclonic flow carries moist air off of the western Panthalassic Ocean onto the continent, but during summer, continental heating generates cyclonic flow, producing monsoon winds that originate over the Tethys Ocean. The result is that intense rains affect southeastern Asia during both seasons. In addition, during summer, the monsoon extends north along Panthalassa, bringing high precipitation to the upper mid-latitude and high-latitude eastern coastline (see Fig. 8a).

#### **Southern Pangaea: The Middle and High Latitudes**

The symmetry of Pangaea, with respect to the equator, and the symmetrical nature of the general circulation on Earth suggest that climates over northern and southern Pangaea would be similar. Certainly, broad similarities do exist. The lack of a bisecting epeiric sea and the distinct orography in the southern hemisphere, however, impart a unique climatic pattern to the southern continent (see Figs. 4–9). As in the northern hemisphere, pressure centers are localized above high topography regions, the winter high pressure cells being shifted poleward from the summer lows. Below-freezing surface-air temperatures extend across most of southern Pangaea during winter, although seasonally averaged coastal temperatures remain above freezing at all latitudes (instantaneous temperatures along high-latitude coasts drop below 0 °C periodically).

The cold temperatures, high pressures, and generally light winds over southern Pangaea in winter create a radiatively and dynamically stable situation that limits moisture exchange during that season. Precipitation contours generally parallel the coastline with higher precipitation amounts along the Tethys where SSTs are warmest. During summer, monsoon circulations are responsible for increases in southern hemisphere precipitation. Cyclonic circulation about the subtropical low in southwestern Pangaea causes surface winds over the western Tethys Ocean to flow southward, where they encroach upon Pangaea in the region of the Indian subcontinent. Precipitation along that coast exceeds

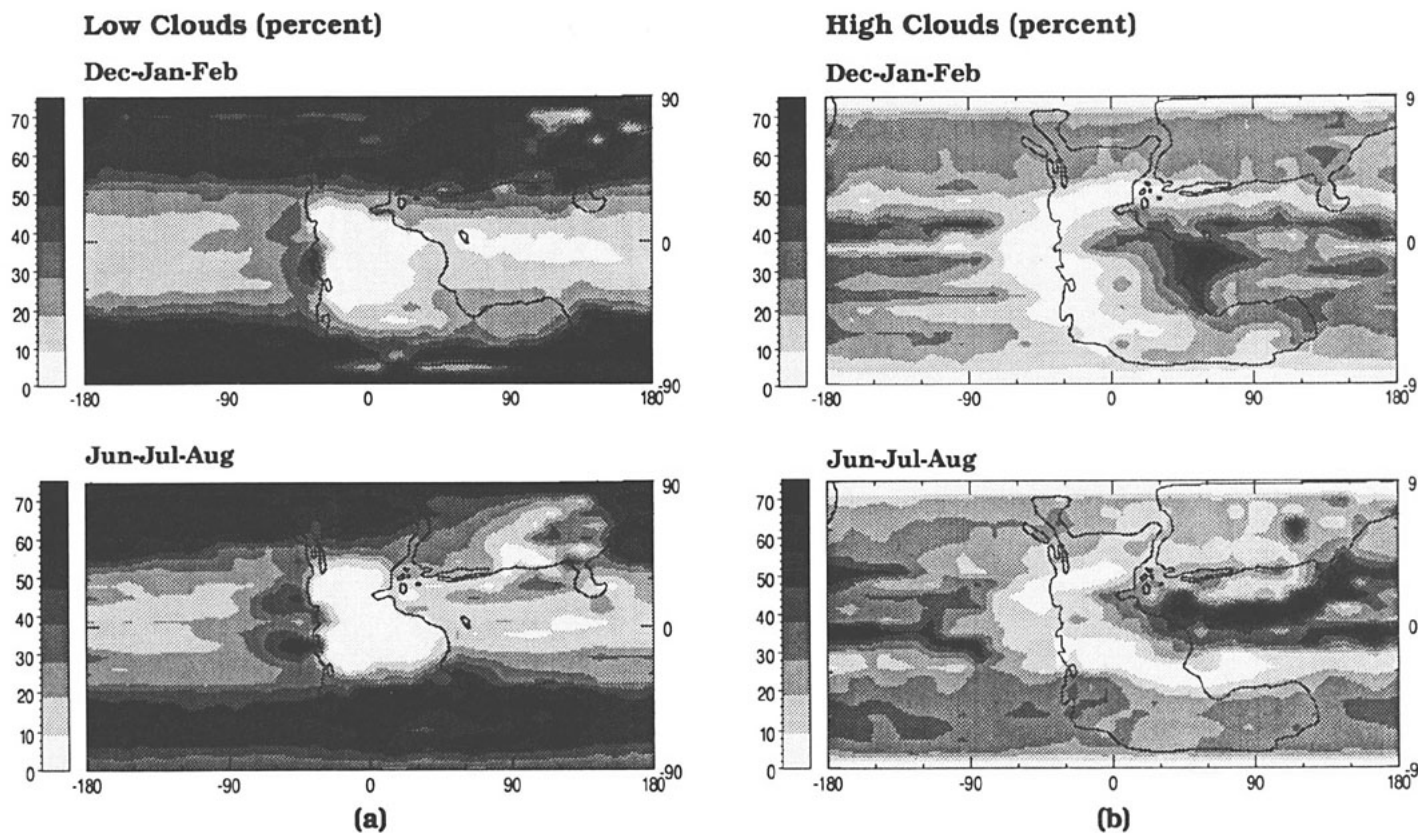


**Figure 7. Simulated global distribution of Early Jurassic cloud cover. (a) Low-level clouds. (b) High-level clouds. The large reduction in the amount of low clouds in the Early Jurassic simulation compared with the present climate represents a positive feedback in a warmer climate. Cloud changes over the tropical continent are particularly conducive to warming because low clouds are reduced while strengthened tropical convection increases higher clouds which trap heat. Cloud cover cannot be validated using the geologic record; however, simulated cloud distributions are critical to an accurate portrayal of climate, as they allow us to understand more fully the reasons for climate changes in the past.**

8 mm/day during summer and, due to the low coastal topography, moisture penetrates well into the southern interior. It is primarily due to this mechanism that the interior region of southern Pangaea receives more precipitation, annually averaged, than does the northern interior. This monsoonal circulation, however, also causes greater seasonal variation in the precipitation field of the southern hemisphere.

Monsoons also affect the easternmost portion of southern Pangaea, again, driven by a summertime low pressure cell. Longshore, westerly winds in the southern Tethys Ocean intersect the continent at its easternmost extent, and strong polar easterlies, turned equatorward by the same low-pressure cell, move inland over the southeastern coast. Not surprisingly, the flow from the warm southern Tethys carries a great deal of moisture, which subsequently condenses, thus increasing low-level cloud cover and precipitation rates over the continent. Winds from the polar ocean, despite their cooler source, also cause a prominent summer precipitation maxi-

mum over southeastern Pangaea, primarily as a result of the uplift of air over coastal mountains.

#### COMPARISONS WITH THE GEOLOGIC RECORD

By virtue of their simplified nature, previous models of Pangaeon climate (Crowley and others, 1989; Kutzbach and Gallimore, 1989) produce results that are not easily compared with the geologic record at the regional level. Rather, they are idealized versions of the Pangaeon climate that can be used to gain insight into supercontinent-type climate processes. The simulation presented here attempts to produce a version of the Early Jurassic climate that, within the limitations of the GCM and the geologic record, is a "possible" Pangaeon climate. Certainly, our simulated climate is not the "true" Early Jurassic climate, because our ability to assign boundary conditions, such as topography and sea-surface temperatures, is limited. Comparisons between results and the geologic rec-

ord, however, are intended as an integral part of this experiment because they help us to recognize points in the simulation that require improvement. Eventually, model results should prove useful for interpreting conflicting geologic signals and for identifying key study sites, as well as allowing us to more fully understand the causes, effects, and feedbacks that are responsible for the paleoclimate record.

#### Surface-Air Temperature Estimates for the Early Jurassic

The large seasonal variation in surface-air temperature simulated over the Early Jurassic continent is not consistent with paleoclimate data predictions for the Mesozoic, a finding that Kutzbach and Gallimore (1989) also noted in their Pangaeon simulation results. Maximum seasonal temperature ranges for the Early Jurassic exceed 45 °C (Fig. 5) over high-latitude continental interiors, a value similar to the present-day seasonality over Siberia. Certainly, such

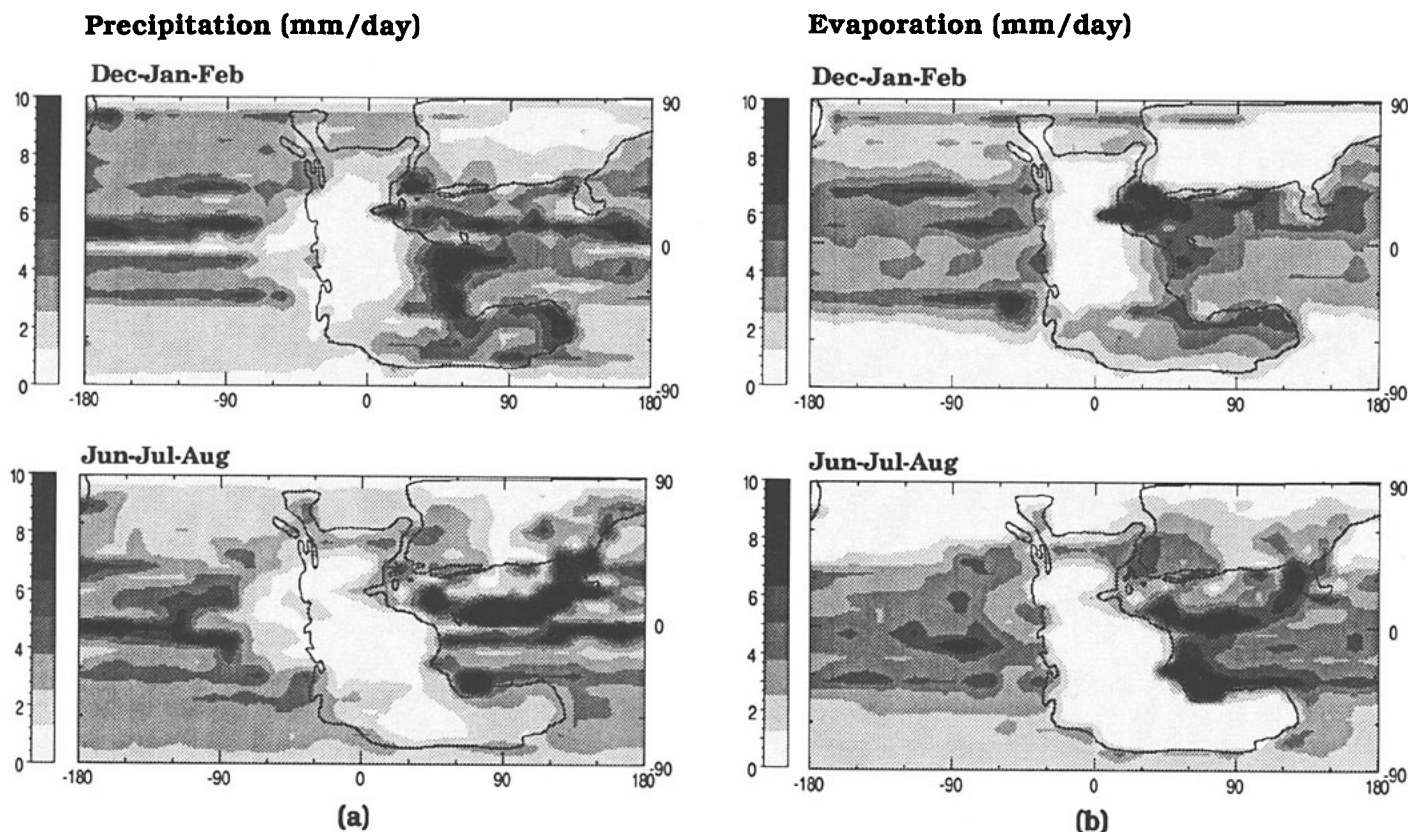


**Figure 8. (a) Precipitation:** simulated global distribution of Early Jurassic precipitation rates. Values below 0.7 mm/day (250 mm/yr) are generally assumed to indicate aridity. Continental regions that receive greater than 4 mm/day of rainfall are found only in regions dominated by monsoon systems. **(b) Evaporation:** simulated global distribution of Early Jurassic rates of evaporation. The primary controls on evaporation are surface heating, wind speed, and moisture availability. Most evaporation therefore occurs over the low-latitude oceans, particularly in regions with warm prescribed SSTs.

extremes are not consistent with the widely held view that Jurassic climates, including those of the continental interior, were equable (Frakes, 1979; Hallam, 1985)

The Jurassic equability hypothesis is supported by fossil evidence for diverse floras as far north as 75°N (Novosibirskiye, Russia) and as far south as 63°S (Grahamland, Antarctica) (Hallam, 1975), and by the fact that warm-water corals extended up to 10° poleward of their present range (Frakes, 1979). These sites, however, are coastal locations, where seasonality would be at a minimum, particularly if SSTs were warmer than at present. Barnard (1973) found some evidence for Early Jurassic continental seasonality in the northern hemisphere floral record, and tree rings in conifers attest to some degree of seasonality (Vakhrameev, 1965, 1991). It is not clear, however, whether the flora are reacting to temperature or moisture changes. In addition, these same authors imply that the degree of seasonality was reduced compared to its present range. Although more paleontological

evidence will improve our understanding of seasonal climate variations, the available data seem to support a reduction in seasonal temperature range over continents for much of Mesozoic and early Cenozoic time (Frakes, 1979; Sloan and Barron, 1990)

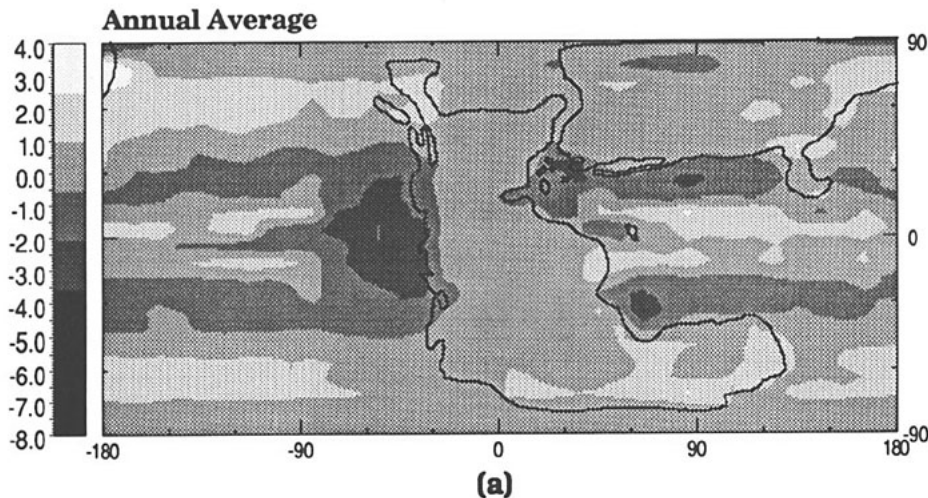
#### Humidity and Aridity in the Early Jurassic

The map of paleoclimate indicators, shown in Figure 2, consists primarily of peat (p) and coal, and evaporite (e) deposits, because they provide the most unequivocal evidence of humid and arid conditions, respectively. Peat and coal deposits imply year-round rainfall and/or low evapotranspiration rates, because a necessary requirement for their formation is persistent wet ground conditions (Hallam, 1984; Parrish, 1988). Evaporites are indicative of environments where the rate of evaporation exceeds that of precipitation plus inflow of water (Gordon, 1975). Restricted marine basins, tidally influenced coastlines, and interior drainage basins

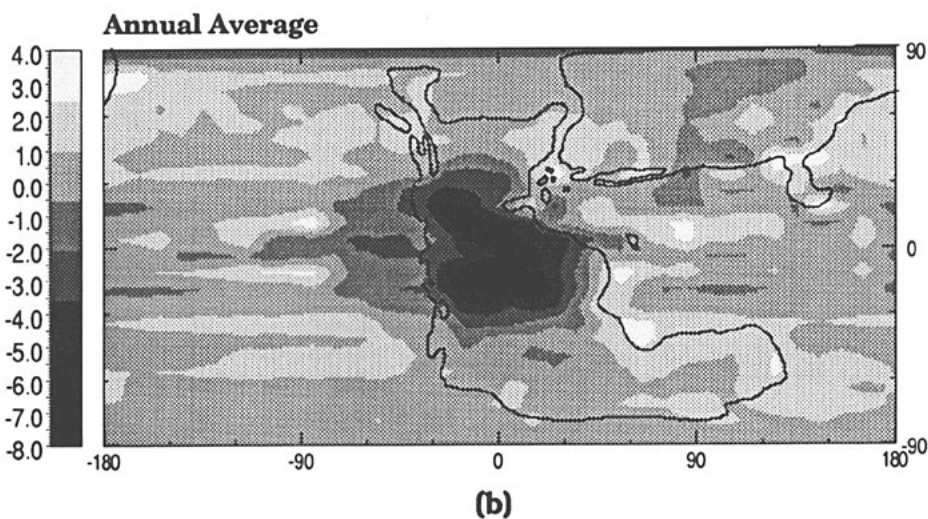
are environments that commonly support evaporite formation. We rely less on other paleoclimate indicators because they are not as easily related to climate variables. Kaolinite dominance in clay-mineral assemblages, and the presence of bauxites and ironstones, however, are generally indicative of humid continental conditions, and eolian deposits suggest continental aridity. Hallam (1984) and Frakes (1979) have given detailed reviews of the paleoclimatic implications of each of these deposits.

Figure 9a shows the annually averaged precipitation minus evaporation ( $p - e$ ) values for the Early Jurassic simulation. Negative values of  $p - e$  are commonly used in paleoclimate modeling studies as a means of identifying arid regions; however, this diagnostic must be viewed with caution. It is actually a proxy for a more accurate definition of aridity, which states that the rate of precipitation minus the *potential* rate of evaporation ( $e_p$ ) must be negative. Unfortunately, GCMs produce values of  $e_p$  over land that are unrealistically large (Delworth and Ma-

## Precipitation minus Evaporation (mm/day)



## Precipitation minus Potential Evaporation (mm/day)



**Figure 9.** (a) Precipitation minus evaporation ( $p - e$ ): simulated global distribution of Early Jurassic annually averaged  $p - e$ . Negative values of  $p - e$  are commonly used to indicate aridity; however, caution must be used when evaluating this value over land in GCM experiments (see discussion in text). (b) Precipitation minus Thornthwaite/GCM Potential Evaporation ( $p - e_{Th}$ ): Values of  $p - e_{Th}$  provide the most accurate representation of moisture balance in GCM paleoclimate simulations.

nabe, 1988; Rind and others, 1990) due, in part, to the lack of realistic vegetation in GCMs. Thus, the model-derived  $p - e_p$  values cannot be used directly to define arid regions. An alternate method, and one which we have found yields a more accurate portrayal of aridity than either of the above methods (Chandler, 1989), uses the model's precipitation minus potential evaporation values that are derived from an empirical bioclimatic formula. We use the bioclimatic

scheme of Thornthwaite (1948) which calculates potential evaporation by using surface-air temperature as its only input. All temperatures are supplied from the GCM simulation. The difference between precipitation and the Thornthwaite/GCM potential evaporation ( $p - e_{Th}$ ) is shown in Figure 9b.

The large-scale pattern of Jurassic aridity and humidity, as derived from this method, is in good agreement with that derived from the pa-

leoclimate record and reported by several authors (Hallam, 1975, 1984, 1985; Parrish and others, 1982; Robinson, 1973). Western Pangaea was extremely arid across the middle and low latitudes, with increasing humidity toward higher latitudes. The eastern sections of Pangaea are more humid, particularly in coastal regions and in regions where monsoon rains dominate. This is similar to the gross pattern found by Kutzbach and Gallimore (1989) using their idealized Pangaeon model. Our simulation differs significantly, however, from their idealized version when regional climatic aspects are evaluated. In the following sections, we present regional comparisons between the geologic data and our simulation results.

**Humid Regions.** High precipitation and positive  $p - e_{Th}$  values (Figs 8a and 9b) indicate that the peat and coal sites in Madagascar, India, and Australia (Gondwana continents), and in Canada, Greenland, Europe, and southeast Asia (Laurasian continents), lie within humid regions. High evaporation rates in the northwest Tethys and across many coastal regions, however, generate negative  $p - e$  values (Figs 8b and 9a) that overlay some coastal coal deposits. The regions in the model which receive year-round rainfall tend to have the largest concentration of major coal deposits. In particular, the region of extensive coal deposition in southeast Asia corresponds very closely with the most humid region of northern Pangaea in our simulation. Minor coal deposits located in Iran (the equatorial island in the western Tethys; see Fig 2) are consistent with the simulation; however, they are probably out of position in our reconstruction because recent evidence suggests that the Iranian microcontinent was probably  $25^\circ$  farther north, adjacent to the northern peninsula (A. M. Ziegler, 1990, personal communication). This new position removes them from their paradoxical location adjacent to major evaporite deposits, yet it still places them in a simulated humid region.

Despite consistency between most of the peat and coal record and the simulated moisture distribution over land, two regions cannot be reconciled with our simulation. One site, in Mexico, lay on the equatorial Panthalassic coast during the Early Jurassic. The second, in central Asia, was located in the interior of north-central Pangaea. The coal deposits in Mexico (Erben, 1957) lie in a zone where the simulated precipitation rate is  $\sim 2$  mm/day; however, high evaporation rates result in negative  $p - e$  and  $p - e_{Th}$  balances (see Fig 9b), indicating that the environment was probably arid despite the rainfall. These coal deposits are minor and may represent nothing more than a local climate or depositional environment anomaly. Nevertheless, their position on the west coast and on the equator

suggests another possible explanation. Ziegler and others (1987) stressed the importance of the overlapping zone of the seasonally migrating ITCZ for maintaining year-round wet conditions and potential coal-forming environments. In our simulation, the ITCZ makes large excursions over the continent and therefore has virtually no overlap zone except for a small area that exactly corresponds to the position of the Mexican coals (see Fig. 4a). Slightly higher precipitation rates in this region compared to surrounding regions probably result from ITCZ and coastal orographic influences. The inability of the GCM to simulate this region as humid, however, probably results from the coarse grid size of our model, which diffuses the ITCZ and smooths orography.

The peat deposits in central Asia are more problematic because they lie within an extensive arid region far from the tropics. These are major coal deposits and are difficult to explain in an arid environment. As topography focuses the monsoons away from this area and also blocks moisture advection from the east, west, and south, it seems possible that the dry interior conditions simulated for northern Pangaea may result from overestimating elevations of mountains in the north. In a sensitivity experiment in which we set the topography equal to 10 m everywhere, the moisture reaching the coal-forming regions of the continental interior was found to increase. Removing the orographic influence, however, also reduced the land-sea pressure differential which reduced the seasonal monsoons and resulted in a decrease in precipitation across the far eastern half of the continent, leaving that region drier than would be expected considering its significant peat deposits.

We suggest that another possible reason for the deposition of the central Asian peat deposits (as well as other interior coals) is the presence of inland bodies of water which are not accounted for in the coarse grid scale of the GCM. The peats themselves suggest the presence of moist ground conditions, and lakes or swamps might have been maintained by runoff from heavy precipitation and snow melt in the mountains to the east. Although ancient drainage patterns are uncertain, the reconstructed topography implies that much of northern Pangaea may have drained interiorly. When we calculated the moisture balance (MB = the sum of precipitation + surface runoff - evaporation) for the central lowlands of the northern peninsula, we found that the moisture surplus in the interior of northern Pangaea is 20.7 mm/day. Calculations of the moisture balance using the Thornthwaite/GCM potential evaporation in place of evaporation still show that the annually averaged moisture surplus is almost 15 mm/day, sufficient to maintain standing water under nearly any drainage conditions.

**Arid Regions.** Perhaps the best known stereotype of the Jurassic climate is that it was extremely arid. This hypothesis is based on the large volume and areal coverage of Jurassic evaporite deposits (Gordon, 1975), eolian sandstones (Blakey and others, 1988), and on qualitative and quantitative models of the Jurassic climate (Hallam, 1985; Kutzbach and Gallimore, 1989; Parrish and others, 1982). Most authors attribute the aridity to the vastness of the supercontinent and its relative position in the trade-wind belt. Yet, the greatest expanse of evaporites are Middle and Late Jurassic in age and were deposited long after the breakup of Pangaea had begun (see Hallam, 1984, for a discussion of this paradox). In fact, the Late Triassic and Early Jurassic were relatively less arid than surrounding time periods. Adding to the curiosity of Early Jurassic aridity is the fact that the median latitude of evaporite deposition was 15°, nearer to the equator than the present 35° (Gordon, 1975), indicating that significant evaporite deposition occurred in a zone that is currently humid.

The highest concentration of Early Jurassic evaporites are found in north Africa, northeastern North America, and Saudi Arabia, where they were formed in lakes, restricted marine basins, and sabkha environments surrounding the western Tethys Ocean. Throughout most of these regions, our simulation confirms the widely held view of extreme tropical and subtropical aridity during the Early Jurassic. By all definitions, most of western Pangaea equatorward of 35° is extremely arid, whereas the region surrounding the northwest Tethys, despite receiving heavy precipitation, has even higher simulated evaporation rates, yielding negative  $p - e$  and  $p - e_{Th}$  values on an annually averaged basis (see Fig. 9). The expansive eolian deposits of the southwestern United States and those in the Bay of Fundy region also lie within the simulated arid region, as do ancient dune deposits in southern Africa. In addition, simulated surface winds over the Early Jurassic southwestern United States are consistent with measurements taken by Peterson (1988) of paleowind directions from cross-strata (compare with Figs. 13 and 14 in Parrish and Peterson, 1988).

The most severe inconsistency between our simulation and the paleoclimate record occurs along the tropical Tethys coast, south of the equator, where extensive Saudi Arabian evaporites provide conclusive evidence for low-latitude aridity. In this region, our simulation shows that high precipitation rates result from both summer and winter monsoons. The strength of the monsoon rains is partially related to the size of the Gondwanan Plateau, bringing into question the prescribed 1,000-m elevation of the plateau. Our 10-m topography sensitivity experiment (mentioned above) shows reduced rainfall

in the region, but the reduction is not sufficient to generate negative  $p - e$  or  $p - e_{Th}$  values. Overestimated SSTs along the coast may also be responsible for the high precipitation rates. Scotese and Summerhayes (1986) predicted that ocean upwelling could have occurred along this coast, which suggests that offshore waters may have been much cooler. As the moisture for this region is derived almost entirely from the east, cooler coastal waters would reduce local convection and the amount of moisture in the air to the east, thus reducing coastal rainfall amounts. Similar scenarios in the current climate affect the Namib and Peru-Chile desert regions. In a sensitivity experiment we reduced the sea-surface temperatures by 2 °C in the coastal grid boxes of the southwest Tethys and found that the  $p - e$ , annually averaged, over the entire coast decreased 1.2 mm/day. Local decreases were up to 3.2 mm/day. Both changes were enough to yield negative  $p - e$  values for the region.

Finally, it is important to note that, although continental aridity was apparently higher than average during the Jurassic, the Earth as a whole was probably less arid. We would expect the warmer atmosphere to hold more moisture, and our simulation indicates that this is the case (see Table 2). Increased evaporation over the oceans leads to an equivalent precipitation increase globally. We find that global precipitation increases by 0.15 mm/day compared to the current climate. The relatively small absolute rainfall values over land, however, imply that continental aridity is aided by a reduction in the transfer of moisture from ocean to land. This conclusion is not surprising, because many authors have hypothesized that a supercontinent would be drier due to the decreased coastal perimeter. It is important to note that, had monsoonal activity not increased precipitation dramatically in some regions, the continent would have been much drier on the average. Considering the intensity of the humidity in regions dominated by monsoons, and the intensity of the aridity in other regions, Pangaea clearly experienced severe geographic extremes of climate in the Early Jurassic. As with surface-air temperature results, therefore, the hydrological cycle results suggest that the character of the Early Jurassic climate is not one of equability.

#### Discussion: The "Equable" Nature of the Early Jurassic Climate

The well-documented occurrence of vast evaporite deposits as well as thick coal deposits on Pangaea suggest that few would refute the claim that Jurassic climates were not "equable" with respect to moisture conditions. The discrepancy between air temperatures interpreted from the geologic record and those simulated in climate models continue to be a subject of in-

tense debate (see Sloan and Barron, 1990). In addition to our Jurassic simulation, Permian, Triassic, Cretaceous, and Eocene simulations have all found extreme continental seasonality (Barron and Washington, 1982b; Fleming, 1983; Crowley and others, 1989; Kutzbach and Gallimore, 1989; Sloan and Barron, 1990), and these experiments span four different climate models. On the other hand, paleoclimate data from the continental interiors, although sparse, include crocodiles and subtropical paleofloras (Lefeld, 1971; MacGinitie, 1974; Wolfe, 1978; P. Markwick, unpub. data), which are difficult to equate with the climates indicated by models.

How then can we explain the apparent contradiction between the paleoclimate data and climate-model results? If the continental interior climates truly were equable, then climate models must (1) lack a fundamental physical process or (2) lack the appropriate boundary conditions for modeling the continental climates of the past. Although the modeling of physical processes in GCMs will certainly undergo improvement during the next decade, there are not any foreseeable additions to their forcing and feedback factors that will influence continental interior climates dramatically. Sensitivity tests exist with developmental versions of the GISS GCM which include coupled ocean models, more detailed ground hydrology routines, more complex cloud parameterizations, and finer resolution grids, yet they do not dramatically change the sensitivity of continental interior temperatures (Rind, 1987b; GISS climate group, 1990, 1991, unpub. results). Furthermore, current GCMs generate generally realistic continental interior temperatures for the present-day climate, implying that, if the problem lies with the models, it is probably related to uncertainties in paleo-boundary conditions. Following the same reasoning, Sloan and Barron (1990) designed several experiments to investigate the sensitivity of the Eocene climate to altered boundary conditions in a GCM. They found that subfreezing winter temperatures over the continents were largely insensitive to changes in either the sea-surface temperature gradient or topography. We found similar results for the Early Jurassic climate, using numerous combinations of boundary conditions in the GISS GCM. Table 3 describes several of our Early Jurassic sensitivity experiments and lists their resulting temperature diagnostics. Notably, none of the experiments produced average winter temperatures that were above freezing. Two simulations, one with extremely warm polar SSTs and one with a large "hypothetical" interior lake, generated the warmest continental interiors, emphasizing the importance of the low continental heat capacity in amplifying the cold continental temperatures. The increased CO<sub>2</sub> simulations reveal that trace gases have little direct effect on continental

warmth; six times the present-day CO<sub>2</sub> yielded a minor temperature increase in the continental interior of 2.3 °C. Warming caused by CO<sub>2</sub> increase results, primarily, from climate feedbacks such as SST warming, sea-ice decrease, and cloud changes. In the Early Jurassic simulations, those feedbacks were previously instigated by the warm specified SSTs and are therefore unavailable to warm the climate further. Net radiation changes show that small increases would occur if SSTs were allowed to adjust (see the method described above). The additional warming, however, is on the order of 1–2 °C, far below the warming needed to create "equable" continental interiors.

Although our experiments show that up to six times the present CO<sub>2</sub> together with increased ocean heat transports was not sufficient to account for seasonal temperature variations, the results are in the right direction, suggesting that more experiments with these major forcing factors are warranted. Such experiments, if aimed at studying regional effects, must be conducted using GCMs which explicitly include CO<sub>2</sub> in their radiation schemes, because models which adjust SSTs or solar irradiance to simulate the CO<sub>2</sub> greenhouse effect create unrealistic forcing patterns, limiting their use in climate interpretation (see Hansen and others, 1984, for examples of the differences). The reduced seasonality in northern Pangaea near the epeiric seaway confirms the importance of inland bodies of water

in regulating continental climates and suggests that lakes and wetlands, which have not been represented in this (or other) paleoclimate simulations, are potentially important in damping the seasonal temperature fluctuations. To the extent that model development allows, such boundary conditions should be included in future simulations.

Although the mystery of equable continental interiors remains, we suggest that the level of disagreement between GCMs and the geologic record has been exaggerated. Micro-environments, such as along inland bodies of water and in valleys, could have harbored many of the paleofloras and faunas in regions with harsh climates, just as they do today. These environments have high potential preservation rates, biasing the geologic record toward climatically sheltered localities. Models, using as they do coarse resolutions, yield climatic averages over vast regions and tend to wash-out micro-environments, describing instead regional-scale climate patterns. The fact that lifeforms, especially animals, seek out climatically favorable, preferentially preserved environments makes them less useful for validating paleoclimate simulations than for validating current climate runs. Detailed paleophytogeography will probably provide the best hope for gaining insights into the questions of continental-interior climates. Plants can yield information about moisture availability as well as temperature conditions,

TABLE 3. SURFACE-AIR TEMPERATURE RESULTS FROM SEVERAL GISS GCM SIMULATIONS

Climate simulation description	Annual average surface air temperature (°C)		Winter only surface air temperature (°C)		High-latitude continental interior
	Land and ocean	Land only	Land and ocean	Land only	
Current climate control	14.3	9.1	10.1	0.9 <sup>†</sup>	-19.2*
Early Jurassic control	18.7	13.6	14.6	2.9	-14.5
E. Jurassic w/ 2 × CO <sub>2</sub>	19.0	14.3	14.8	3.5	-13.8
E. Jurassic w/ 4 × CO <sub>2</sub>	19.2	15.1	15.0	4.0	-12.9
E. Jurassic w/ 6 × CO <sub>2</sub>	19.4	15.5	15.2	4.6	-12.2
E. Jurassic w/ uniform 10-m elevation	19.2	15.5	15.1	4.8	-12.6
E. Jurassic w/ uniform vegetation	18.8	13.8	14.7	3.1	-13.9
E. Jurassic w/ 10 °C polar SSTs	20.2	15.2	16.0	4.3	-12.0
E. Jurassic w/ 20 °C polar SSTs	22.2	18.2	18.1	8.1	-7.5
E. Jurassic w/ continental interior lake in north Pangaea	18.8 <sup>†</sup>	12.9 <sup>†</sup>	14.7 <sup>†</sup>	3.7 <sup>†</sup>	-8.8 <sup>†</sup>

<sup>†</sup>Values are for the northern hemisphere only.

\*Values for the current climate simulation are from the Siberian Plateau, values for the Early Jurassic simulations are from the high-latitude interiors of northern and southern Pangaea.

and have the unique ability to give us information about seasonal conditions. Preliminary bioclimatic interpretations based on detailed paleophytogeography (Y. Jiping and A. M. Ziegler, 1991, personal commun.) suggest that the 0 °C isotherm in northern Pangaea (data from China) during Early Jurassic time is located near the position described by our simulation. In addition, A. M. Ziegler has suggested (1991, personal commun.) that the paleoflora described by Vakhrameev (1991) from central Asian localities are primarily cold temperate varieties. For comparison, Chicago, Illinois, has a modern climate that falls into the cold temperate category and has average winter temperatures of approximately -2 °C. Clearly, such climates cannot be considered equable. If Ziegler's interpretation is correct, the winter-time surface-air temperatures in the continental interior of Jurassic Pangaea were not as warm as has been previously suggested.

#### SUMMARY AND CONCLUDING REMARKS

The major features of the simulated Early Jurassic climate include warm surface-air temperatures, extreme continental aridity in the low and middle latitudes of western Pangaea, and monsoons which dominate along the mid-latitude coasts of Tethys and Panthalassa and which also affect conditions deep into the continental interiors in some regions. The GCM results are supported by the distribution of most coals and peats, evaporites, eolian deposits, and high-latitude fossil floras. The greatest mismatch occurs along the low-latitude Tethys coast, where the GCM simulates wet conditions over what is now Saudi Arabia, and which was, in early Jurassic time, a region covered by evaporites. Sensitivity experiments suggest that the inclusion of cooler waters along the southwest Tethys coast (simulating a zone of deep-water upwelling) generates a drier climate along that coast and is a likely candidate to solve the problem.

Like other pre-Pleistocene simulations, the Early Jurassic shows large seasonal temperature ranges within the continental interiors. We experimented with variations in topography, sea-surface temperature, vegetation, and atmospheric CO<sub>2</sub> content, and we discovered that none of the scenarios yielded continental interiors in which winter temperatures remained above freezing everywhere. As we also found that moisture availability is highly variable and dependent upon geographic factors, we conclude that neither the temperature nor the moisture results support the concept of an equable Jurassic climate.

The most important finding from our simulation is that the warm climate of the Early Jurassic could be maintained without additional forcing from CO<sub>2</sub>. Starting our simulation with warm high-latitude SSTs implicitly provided the model with increased ocean heat transports. Those heat transports instigated several positive feedbacks that supported the warmer system, yielding an Early Jurassic climate that equilibrates at much warmer temperatures than the current climate. Our simulation does not address the question of why the ocean heat transports might have been greater, although calculations show that an increase of only 42% would create an SST distribution like the one we specified (Rind and Chandler, 1991). Our simulation does indicate that, when established, increases in sea-surface and atmospheric temperatures could be maintained even if the initiating forces were removed. If true, we must consider the possibility that short-term changes in ocean circulation may have resulted in long-term climatic warming. The implications for Mesozoic climates, as well as for future climates, are considerable.

The first responsibility of a paleoclimate simulation is to duplicate the climatic patterns established from the paleoclimate record. We have attempted to achieve this goal within the limitations of the known boundary conditions and the current state of GCM development. The majority of the comparisons show that the Early Jurassic simulation agrees with the sedimentary paleoclimate data; however, the limitations lead to some discrepancies. We have tried to focus on the contrasts, discussing possible explanations for the mismatches. There are inherent difficulties involved in comparing GCM results with geologic data, especially in the case of paleoclimate modeling, where we rely on uncertain boundary conditions interpreted from an incomplete record. Certainly there is the potential for circularity in our interpretations, because we use the same record to both initiate and validate the model. The exercise, however, is not a futile one. Three-dimensional models such as GCMs are based, as much as possible, on fundamental principles of physics; thus the results they generate are based only partly on boundary conditions. This is the main reason for using a three-dimensional climate model to simulate paleoclimates; models that rely heavily on parameterizations (approximations of physical processes), such as 2-D energy-balance models, are extremely limited in their ability to examine the full range of forces and feedbacks that constitute climate. GCMs also use parameterizations for some important processes, such as ocean circulation and cloud formation, and, no matter how detailed those parameterizations become, they

are nonetheless the weakest points of the models. They are also the topics which are receiving the most attention from model developers.

It seems appropriate to ask any climate model to supply more information than could be obtained from a reasonably well educated interpretation of available data. For paleoclimate study, the most obvious advantages of the model include its quantitative ability and its ability to supply information for regions that lack or have confusing paleoclimate data. In addition, the model can supply values for a vast array of climate variables that are probably impossible to estimate from paleoclimate data. Many of these variables, particularly those that describe atmospheric dynamics and energy-transfer relationships, are critical to a complete understanding of past climates. We have attempted to touch on a few of these aspects of the modeled climatology, concentrating on features that are critical components of the climate system. To fully utilize the voluminous data produced by the state-of-the-art climate models, paleoclimatologists will be required to gain a significant understanding of the atmospheric sciences as well as a better understanding of the models themselves and their limitations.

#### ACKNOWLEDGMENTS

We gratefully acknowledge A. M. Ziegler and the Paleogeographic Atlas Project group at the University of Chicago for their help in constructing the boundary conditions used in the simulation. Discussions with N. Christie-Blick, P. Olsen, J. Hays, and J. Kutzbach were very helpful during the comparison between model results and the geologic record. Comments by J. T. Parrish, E. Barron, and an anonymous reviewer helped us to improve the manuscript.

#### REFERENCES CITED

- Abramopoulos, F., Rosenzweig, C., and Choudhury, B., 1988, Improved ground hydrology calculations for global climate models (GCMs): Soil water movement and evapotranspiration: *Journal of Climate*, v. 1, p. 921-941.
- Arkell, W. J., 1956, *Jurassic geology of the world*: Edinburgh, Scotland, Oliver and Boyd Ltd., 806 p.
- Arthur, M. A., Dean, W. E., and Schlanger, S. O., 1985, Variations in the global carbon cycle during the Cretaceous related to climate, volcanism, and changes in atmospheric CO<sub>2</sub>, in Sundquist, E. T., and Broecker, W. S., eds., *The carbon cycle and atmospheric CO<sub>2</sub>: Archean to present*: American Geophysical Union Geophysical Monograph 32, p. 504-530.
- Barnard, P.D.W., 1973, *Mesozoic floras*, in Hughes, N. F., ed., *Organisms and continents through time*: Oxford, England, Paleontological Society of London, Blackwell, p. 175-188.
- Barron, E. J., 1980, *Paleogeography and climate 180 million years to present* [Ph.D. dissert.]: Miami, Florida, University of Miami, 280 p.
- , 1985, *Climate models: Applications for the pre-Pleistocene*, in Hecht, A. D., ed., *Paleoclimate analysis and modeling*: New York, Wiley, p. 397-431.
- , 1987, *Eocene equator-to-pole surface ocean temperatures: A significant climate problem?* *Paleoceanography*, v. 2, p. 729-739.
- Barron, E. J., and Washington, W., 1982a, *Atmospheric circulation during warm geologic periods: Is the equator-to-pole surface-temperature gradient the controlling factor?* *Geology*, v. 10, p. 633-636.
- , 1982b, *Cretaceous climate: A comparison of atmospheric simulations with the geologic record*: *Paleogeography, Palaeoclimatology, Palaeoecology*, v. 40, p. 103-133.

- 1984, The role of geographic variables in explaining paleoclimates: Results from Cretaceous climate model sensitivity experiments: *Journal of Geophysical Research*, v. 89, p. 1267–1279.
- 1985, Warm Cretaceous climates: High atmospheric CO<sub>2</sub> as a plausible mechanism, in Sundquist, E. T., and Broecker, W. S., eds., The carbon cycle and atmospheric CO<sub>2</sub>: Natural variations Archaean to present: Washington, D.C., American Geophysical Union Geophysical Monograph 32, p. 546–553.
- Barron, E. J., Thompson, S., and Schneider, S., 1981, An ice-free Cretaceous? Results from climate model simulations: *Science*, v. 212, p. 501–508.
- Bates, R. L., and Jackson, J. A., 1980, Glossary of geology: Falls Church, Virginia, American Geological Institute, 751 p.
- Berner, R. A., and Landis, G. P., 1987, Chemical analysis of gaseous bubble inclusions in amber: The composition of ancient air? *American Journal of Science*, v. 287, p. 757–762.
- Blakey, R. C., Peterson, F., and Kocurek, G., 1988, Synthesis of late Paleozoic and Mesozoic eolian deposits of the Western Interior of the United States: *Sedimentary Geology*, v. 56, p. 3–125.
- Bradley, R. S., 1985, Quaternary paleoclimatology: Methods of paleoclimate reconstruction: Boston, Massachusetts, Allen and Unwin, 472 p.
- Brenchley, P. J., 1984, Fossil and climate: Chichester, England, John Wiley & Sons, 352 p.
- Chandler, M., 1989, Jurassic climate simulations using the GISS GCM: Aridity in a warmer climate [abs.]: *Eos (American Geophysical Union Transactions)*, v. 70, p. 1010.
- COHMAP (Cooperative Holocene Mapping Project) Project Members, 1988, Climatic changes of the last 18000 years: Observations and model simulations: *Science*, v. 241, p. 1043–1052.
- Covey, C., 1991, Climate change: Credit the oceans? *Nature*, v. 352, p. 196–197.
- Crowley, T. J., 1983, The geologic record of climatic change: Reviews of Geophysics and Space Physics, v. 21, p. 828–877.
- Crowley, T. J., Mengel, J. G., and Short, D. A., 1987, Gondwanaland's seasonal cycle: *Nature*, v. 329, p. 803–807.
- Crowley, T. J., Hyde, W. T., and Short, D. A., 1989, Seasonal cycle variations on the supercontinent of Pangaea: *Geology*, v. 17, p. 457–460.
- Delworth, T., and Manabe, S., 1988, The influence of potential evaporation on the variabilities of simulated soil wetness and climate: *Journal of Climate*, v. 1, p. 523–547.
- Dickinson, R. E., 1984, Modeling evapotranspiration for three-dimensional global climate models, in Hansen, J. E., and Takahashi, T., eds., Climate processes and climate sensitivity: Washington, D.C., American Geophysical Union Geophysical Monograph 29, Maurice Ewing Volume 5, p. 58–72.
- Doyle, P., 1987, Lower Jurassic–Lower Cretaceous Belemnite biogeography and the development of the Mesozoic boreal realm: *Paleogeography, Paleoclimatology, Paleoecology*, v. 61, p. 237–254.
- Druyan, L. M., 1982a, Studies of the Indian summer monsoon with a coarse-mesh general circulation model, Part I: *Journal of Climatology*, v. 2, p. 127–139.
- 1982b, Studies of the Indian summer monsoon with a coarse-mesh general circulation model, Part II: *Journal of Climatology*, v. 2, p. 347–355.
- Emmanuel, W. R., Shugart, H. H., and Stevenson, M. P., 1985, Climate change and the broad-scale distribution of terrestrial ecosystem complexes: *Climatic Change*, v. 7, p. 29–43.
- Erben, H. K., 1957, Paleogeographic reconstructions for the Lower and Middle Jurassic and for the Callovian of Mexico, 20th International Geological Congress of Mexico, Report, Section 11, p. 35–40.
- Filatoff, J., 1975, Jurassic palynology of the Perth Basin, western Australia: *Palaentographica, Abteilung B*, v. 154, p. 1–113.
- Fleming, J. C., 1983, Late Cretaceous climate simulation using GISS model II general circulation model: Summer Institute Research Project, Summer Institute for Planets and Climate, sponsored by Columbia University in conjunction with NASA GISS, p. 19 [available from M. Chandler].
- Frakes, L. A., 1979, Climate throughout geologic time: Amsterdam, The Netherlands, Elsevier, 310 p.
- Frakes, L. A., and Francis, J. E., 1988, A guide to Phanerozoic cold polar climates from high-latitude ice-rafting in the Cretaceous: *Nature*, v. 333, p. 547–549.
- Glennie, K. W., 1987, Desert sedimentary environments, present and past—A summary: *Sedimentary Geology*, v. 50, p. 135–165.
- Gordon, W. A., 1975, Distribution by latitude of Phanerozoic evaporite deposits: *The Journal of Geology*, v. 83, p. 671–684.
- Hallam, A., 1975, Jurassic environments: Cambridge, England, Cambridge University Press, 269 p.
- 1984, Continental humid and arid zones during the Jurassic and Cretaceous: *Paleogeography, Paleoclimatology, Paleoecology*, v. 47, p. 195–223.
- 1985, A review of Mesozoic climates: *Geological Society of London Journal*, v. 142, p. 433–445.
- Hansen, J., Johnson, D., Lacs, A., Lebedeff, S., Lee, P., Rind, D., and Russell, G., 1981, Climate impact of increasing atmospheric carbon dioxide: *Science*, v. 213, p. 957–966.
- Hansen, J. E., Russell, G., Rind, D., Stone, P., Lacs, A., Lebedeff, S., Ruedy, R., and Travis, L., 1983, Efficient three-dimensional global models for climate studies: Models I and II: *Monthly Weather Review*, v. 111, p. 609–662.
- Hansen, J. E., Lacs, A., Rind, D., Russell, G., Stone, P., Fung, I., Ruedy, F., and Lerner, J., 1984, Climate sensitivity: Analysis of feedback mechanisms, in Hansen, J. E., and Takahashi, T., eds., Climate processes and climate sensitivity: Washington, D.C., American Geophysical Union, p. 130–163.
- Harland, W. B., Armstrong, R. L., Cox, A. V., Craig, L. E., Smith, A. G., and Smith, D. G., 1990, A geologic time scale 1989: Cambridge, England, Cambridge University Press.
- Holton, J. R., 1979, An introduction to dynamic meteorology: Orlando, Florida, Academic Press, 391 p.
- Hubert, J. R., and Mertz, K. A., 1984, Eolian sandstones in Upper Triassic–Lower Jurassic red beds of the Fundy Basin, Nova Scotia: *Journal of Sedimentary Petrology*, v. 54, p. 798–810.
- Hughes, N. F., 1973, Mesozoic and Tertiary distributions, and problems of land-plant evolution, in Hughes, N. F., ed., Special Papers in Paleontology No. 12: Oxford, England, Paleontological Society of London, Blackwell, p. 189–190.
- Kocurek, G., and Dott, R. H., Jr., 1983, Jurassic paleogeography and paleoclimate of the central and southern Rocky Mountains region, in Reynolds, M. W., and Dolly, E. D., eds., Mesozoic paleogeography of the west-central United States: Denver, Colorado, Society of Economic Paleontologists and Mineralogists, Rocky Mountain Section, p. 101–116.
- Kutzbach, J. E., and Gallimore, R. G., 1989, Pangaea climates: Megamontoons of the megacontinent: *Journal of Geophysical Research*, v. 94, p. 3341–3357.
- Kutzbach, J. E., and Guetter, P. J., 1986, The influence of changing orbital parameters and surface boundary conditions on climate simulations for the past 18000 years: *Journal of the Atmospheric Sciences*, v. 43, p. 1726–1759.
- Kutzbach, K. E., and Street-Perrott, F. A., 1985, Milankovitch forcing of fluctuations in the level of tropical lakes from 18 to 0 kyr BP: *Nature*, v. 317, p. 130–134.
- Lefeld, J., 1971, Geology of the Djadokhta Formation at Bayn Dzak (Mongolia): *Palaentographica Polonica*, v. 25, p. 101–127.
- MacGinitie, H. D., 1974, An early middle Eocene flora from the Yellowstone-Absaroka volcanic province, northwestern Wind River Basin, Wyoming: University of California Publications, Geological Sciences, v. 108, p. 1–103.
- Manabe, S., and Broccoli, A. J., 1985, The influence of continental ice sheets on the climate of an ice age: *Journal of Geophysical Research*, v. 90, p. 2167–2190.
- Manabe, S., and Bryan, K., Jr., 1985, CO<sub>2</sub>-induced change in a coupled ocean-atmosphere model and its paleoclimatic implications: *Journal of Geophysical Research*, v. 90, p. 11689–11707.
- Matthews, E., 1984, Prescription of land-surface boundary conditions in GISS GCM II: A simple method based on high-resolution vegetation data bases: NASA Goddard Space Flight Center Institute for Space Studies, NASA Technical Memorandum 86096, 20 p.
- 1985, Atlas of archived vegetation, land-use and seasonal albedo data sets: NASA Goddard Space Flight Center Institute for Space Studies, NASA Technical Memorandum 86199, 53 p.
- Newman, M. J., and Rood, R. T., 1977, Implications of solar evolution for the Earth's early atmosphere: *Science*, v. 198, p. 1035–1037.
- Ogelsby, R., and Park, J., 1989, The effect of precessional insolation changes on Cretaceous climate and cyclic sedimentation: *Journal of Geophysical Research*, v. 94, p. 14,793–14,816.
- Olsen, P. E., 1986, A 40-million-year lake record of Early Mesozoic orbital climatic forcing: *Science*, v. 234, p. 842–848.
- Overpeck, J., Jacoby, G., Rind, D., Bradley, R. S., Thompson, L. G., and Mosley-Thompson, E., 1989, Analysis of rapid and recent climate change: Proposal to the National Science Foundation, Division of Climate Dynamics, p. 141.
- Paleogeographic Atlas Project, 1991, University of Chicago, Department of the Geological Sciences, Project Director, A. M. Ziegler.
- Parrish, J. T., 1985, Latitudinal distribution of land and shelf and absorbed solar radiation during the Phanerozoic: U.S. Geological Survey Open-File Report 85-31, 21 p.
- 1988, Controls on the distribution of Cretaceous coals—An overview: *Geological Society of America Abstracts with Programs*, v. 20, p. A27.
- Parrish, J. T., and Peterson, F., 1988, Wind directions predicted from global circulation models and wind directions determined from eolian sandstones of the western United States—A comparison: *Sedimentary Geology*, v. 56, p. 261–282.
- Parrish, J. T., Ziegler, A. M., and Scotese, C. R., 1982, Rainfall patterns and the distribution of coals and evaporites in the Mesozoic and Cenozoic: *Paleogeography, Paleoclimatology, Paleoecology*, v. 40, p. 67–101.
- Peterson, F., 1988, Pennsylvanian to Jurassic eolian transportation systems in the western United States: *Sedimentary Geology*, v. 56, p. 207–260.
- Ramanathan, V., Barkstrom, B. R., and Harrison, E. F., 1989a, Climate and the Earth's radiation budget: *Physics Today*, v. 42, May, p. 22–32.
- Ramanathan, V., Cess, R. D., Harrison, E. F., Minnis, P., Barkstrom, B. R., Ahmad, E., and Hartmann, D., 1989b, Cloud-radiative forcing and climate: Results from the Earth Radiation Budget Experiment: *Science*, v. 243, p. 57–63.
- Raval, A., and Ramanathan, V., 1989, Observational determination of the greenhouse effect: *Nature*, v. 342, p. 758–761.
- Rind, D., 1982, The influence of ground moisture conditions in North America on summer climate as modeled in the GISS GCM: *Monthly Weather Review*, v. 110, p. 1487–1494.
- 1984, The influence of vegetation on the hydrologic cycle in a global climate model, in Hansen, J. E., and Takahashi, T., eds., Climate processes and climate sensitivity: Washington, D.C., American Geophysical Union Geophysical Monograph 29, Maurice Ewing Volume 5, p. 73–91.
- 1986, The Dynamics of warm and cold climates: *Journal of the Atmospheric Sciences*, v. 43, p. 3–24.
- 1987a, Components of the Ice Age circulation: *Journal of Geophysical Research*, v. 92, p. 4241–4281.
- 1987b, The doubled CO<sub>2</sub> climate: Impact of the sea surface temperature gradient: *Journal of the Atmospheric Sciences*, v. 44, p. 3235–3268.
- 1988, The dependence of warm and cold climate depiction on climate model resolution: *Journal of Climate*, v. 1, p. 965–997.
- 1990, The paleorecord: How useful is it in testing models?, in Bradley, R. S., ed., Global changes of the past: Boulder, Colorado, UCAR/Office for Interdisciplinary Earth Studies, p. 397–420.
- Rind, D., and Chandler, M., 1991, Increased ocean heat transports and warmer climate: *Journal of Geophysical Research*, v. 96, p. 7437–7461.
- Rind, D., and Petzet, D., 1985, Terrestrial conditions at the last glacial maximum and CLIMAP sea-surface temperature estimates: Are they consistent? *Quaternary Research*, v. 24, p. 1–22.
- Rind, D., and Rossow, W. B., 1984, The effects of physical processes on the Hadley circulation: *Journal of the Atmospheric Sciences*, v. 41, p. 479–507.
- Rind, D., Petzet, D., Broecker, W., McIntyre, A., and Ruddiman, W., 1986, The impact of cold North Atlantic sea surface temperatures on climate: Implications for the Younger Dryas cooling (11–10 k): *Climate Dynamics*, v. 1, p. 3–33.
- Rind, D., Goldberg, R., Hansen, J., Rosenzweig, C., and Ruedy, R., 1990, Potential evaporation and the likelihood of future drought: *Journal of Geophysical Research*, v. 95, p. 9983–10004.
- Robinson, P. L., 1973, Paleoclimatology and continental drift, in Tarling, D. H., and Runcom, S. K., eds., Implications of continental drift to the Earth sciences: London, England, Academic Press, p. 449–476.
- Ruddiman, W. F., and Kutzbach, J. E., 1989, Forcing of Late Cenozoic northern hemisphere climate by plateau uplift in southeast Asia and the American southwest: *Journal of Geophysical Research*, v. 94, p. 18,409–18,428.
- Schneider, S. H., Thompson, S. L., and Barron, E. J., 1985, Mid-Cretaceous continental surface temperatures: Are high CO<sub>2</sub> concentrations needed to simulate above-freezing winter conditions?, in Sundquist, E. T., and Broecker, W. S., eds., The carbon cycle and atmospheric CO<sub>2</sub>: Archaean to present: Washington, D.C., American Geophysical Union Geophysical Monograph 32, p. 554–560.
- Scotese, C. R., and Summerhayes, C. P., 1986, Computer model of paleoclimate predicts coastal upwelling in the Mesozoic and Cenozoic: *Geobase, Summer Issue*, p. 28–42.
- Shackleton, N., and Boersma, A., 1981, The climate of the Eocene ocean: *Geological Society of London Journal*, v. 138, p. 153–157.
- Sloan, L. C., and Barron, E. J., 1990, "Equable" climates during Earth history?: *Geology*, v. 18, p. 489–492.
- Smith, A. G., and Briden, J. C., 1977, Mesozoic and Cenozoic paleocontinental maps: Cambridge, England, Cambridge University Press, 63 p.
- Stevens, G. R., and Clayton, R. N., 1971, Oxygen isotope studies on Jurassic and Cretaceous belemnites from New Zealand and their biogeographic significance: *New Zealand Journal of Geology and Geophysics*, v. 14, p. 829–897.
- Sud, Y. C., and Smith, E., 1985, The influence of surface roughness of deserts on the July circulation: *Boundary-Layer Meteorology*, v. 33, p. 15–49.
- Termier, H., and Termier, G., 1960, Atlas de Paléogéographie: Paris, France, Masson and Co., 99 p.
- Thornthwaite, C. W., 1948, An approach toward a rational classification of climate: *Geographical Review*, v. 38, p. 55–89.
- Vakhrameev, V. A., 1965, Jurassic floras of the U.S.S.R.: *Paleobotanist*, v. 14, p. 118–123.
- 1991, Jurassic and Cretaceous Floras and Climates of the Earth: Translated by Litvinov, J. V.: Cambridge, England, Cambridge University Press, 318 p.
- Dobrushkina, I. N., Zaklinskaya, E. D., and Meyen, S. V., 1970, Paleozoic and Mesozoic floras of Eurasia and phytogeography of this time: Moscow, Academy of Sciences Geological Institute Trudy, v. 208, p. 1–245.
- Wallace, J. M., and Hobbs, P. V., 1977, Atmospheric science: An introductory survey: Orlando, Florida, Academic Press, 467 p.
- Wesley, A., 1973, Jurassic plants, in Hallam, A., ed., Atlas of Paleobiogeography: Amsterdam, The Netherlands, Elsevier, p. 329–338.
- Wolfe, J. A., 1978, A paleobotanical interpretation of Tertiary climates in the northern hemisphere: *American Journal of Science*, v. 66, p. 691–703.
- Wolfe, J. A., and Upchurch, G. R., 1987, North American nonmarine climates and vegetation during the Late Cretaceous: *Paleogeography, Paleoclimatology, Paleoecology*, v. 61, p. 33–77.
- Ziegler, A. M., Scotese, C. R., and Barrett, S. F., 1983, Mesozoic and Cenozoic paleogeographic maps, in Brosche, P., and Sündermann, J., eds., Tidal friction and the Earth's rotation II: Berlin, West Germany, Springer-Verlag, p. 240–252.
- Ziegler, A. M., Raymond, A. L., Gierlowski, T. C., Horrell, M. A., Rowley, D. B., and Lottes, A. L., 1987, Coal, climate and terrestrial productivity: The present and Early Cretaceous compared, in Scott, A. C., ed., Coal and coal bearing strata: Recent advances: Geological Society of London Special Publication No. 32, p. 25–49.